Volume 46, July/August 2014

ELSEVIER

European Journal of
Mechanics
B/Fluids

Editors-in-Chief: F. Dias, Cachan (France) G.J.F. van Heijst, Eindhoven (Netherlands)

Associate Editors

P. Luchini, Salerno (Italy)

E.H. Meiburg, Santa Barbara (USA)

A. Thess, Ilmenau (Germany)

(Founded in 1961 as Journal de Mécanique)

www.elsevier.com/locate/ejmflu

Laminar boundary-layer separation control by Görtler-scale blowing

L.L. van Dommelen, R. Yapalparvi *

Department of Mechanical Engineering, Florida A&M University – Florida State University College of Engineering, Tallahassee, FL 32310-6046, USA

ARTICLE INFO

ABSTRACT

Recent experimental work has succeeded in retarding or removing boundary-layer separation by means of blowing supersonic microjets transversely through the wall. To provide some theoretical context for such work, the current study examines the removal of separation by transverse blowing within the framework of the standard Prandtl scalings for incompressible boundary layers. One key result, obtained using asymptotic analysis, is that such removal is not possible for two-dimensional flow. Neither is removal of separation possible by three-dimensional blowing in an initially two-dimensional separated boundary layer if the blowing distribution has a finite-scale spanwise variation. The second key result obtained is that the previous conclusion is no longer valid when there is nontrivial short-scale spanwise variation of the blowing distribution. This result is obtained by providing a numerical counter-example in which blowing, with a Görtler scale spanwise variation, creates an attached boundary layer flow where none existed before the blowing. One consequence is that there are at least some flows in which transverse Görtler-scale blowing can turn a separated flow into an attached flow, with a vanishingly small drag that is inversely proportional to the square root of the Reynolds number. The flow physics of the computed example is analyzed to obtain a better understanding of how the Görtler-scale blowing affects the flow.

© 2014 Elsevier Masson SAS. All rights reserved.

1. Introduction

Effective control of boundary-layer separation can have many benefits. For example, avoidance of stall limits helicopter rotor efficiency and performance, especially on the retreating blades in the presence of forward motion. Stall is also a limiting factor for control surfaces of missiles and projectiles. A large number of control mechanisms have been developed, ranging from classical suction and vortex generators to synthetic jets, and some are quite effective. The largest problem is often not efficiency but associated costs and practical application in challenging real-life environments.

A new approach has been proposed recently that promises to be much more robust and effective in applications. Control is achieved by blowing supersonic microjets, with diameters described in microns, into the boundary layer. Experiments for both dynamic stall, [1], and steady separation, [2–6], show that the microjets are effective in eliminating stall and its adverse effects on lifting forces and resistance. These are very promising results, because unlike classical suction, blowing will repel dirt and other contaminants, rather than suck them toward the surface. See [7,8] for more on

such issues. Moreover, sources of high pressure air, such as engine bleed, may readily be found. Because of the micron dimensions, the amount of air required by the microjets is negligible. By its nature, the control can readily be completely removed when no longer needed and it is easily modulated, [9,10].

However, optimizing the location, spacing and distribution of the jets to predict and maximize benefits without prohibitive situation-specific experiments is a significant problem due to a lack of understanding of why the control is effective. While the generation of enhanced streamwise vorticity seems to be a likely mechanism for the beneficial effects, the process is clearly internal to the boundary layer, due to the microscopic size and mass flow rates of the jets, [2–6]. Modeling the process as classical vortex generators that produce organized vortices of significant scale is simply not realistic.

For those reasons, it seems worthwhile to look for a simple model that may explain some of the issues involved in microjet separation control. The simplest reasonable model would seem to be two-dimensional laminar boundary layer flow with distributed boundary-layer scale blowing through the wall. Of course, this model will not describe the precise small-scale features of the flow right at the microjets. However, the actual separation being removed is well downstream of the microjets, where the small scale details of the jets are presumably long diffused out. So the model seems a reasonable starting point. And there is appreciable existing data on the effects of blowing and suction within this model.

* Correspondence to: ANSYS, 10 Cavendish Ct, Lebanon, NH, 03766, USA. Tel.: +1 603-727-5634.
E-mail addresses: dommelen@eng.fsu.edu (L.L. van Dommelen), ramesh.yapalparvi@gmail.com (R. Yapalparvi).

But the first problem now arises immediately. Since the pioneering paper of Prandtl [11] that initiated boundary layer theory, the notion has been established that transverse suction, rather than blowing is needed to remove separation. Indeed, considerable practical experience in two-dimensional laminar boundary layer computations, (e.g. [12,13]), suggests that transverse blowing promotes, rather than prevents, separation.

The question then becomes whether it is even possible, within the two-dimensional model, to remove separation by blowing, regardless of how well the blowing distribution is chosen to simulate microjets. In Section 3 we show that the answer is no. Separation cannot be removed by blowing in a two-dimensional laminar incompressible Prandtl boundary layer.

This result is interesting, because it indicates that microjet flow control is not as trivial as it may seem. (Consistent with that, Vikas Kumar, during his Ph.D. thesis defense noted that it was possible to create separation using microjets where there was none before.) Furthermore, the result generalizes to the statement that using a three-dimensional blowing distribution cannot remove separation either, as long as the distribution has a finite spanwise scale.

However, when the spanwise variation of the blowing distribution becomes sufficiently small, the given analytical arguments that exclude removal of separation are no longer valid. The question becomes then whether it remains impossible to remove separation using transverse blowing on a boundary-layer scale. In Section 6 it is shown by a counter-example that the answer is no. The counter-example removes separation from a slightly concave surface by blowing on a short, Görtler-type, spanwise scale.

The counter-example gives a reasonable qualitative explanation of the experimental results of [2–4] within the simple framework of incompressible laminar boundary layer theory. (Note that the experiments were turbulent.) As discussed in Section 8, considerable further efforts seem to be needed to gain a better understanding of other cases in which microjets have been used.

2. Comments on the definition of separation

One issue that seems to require clarification is what we mean with the terms "separated" and "unseparated" flow. Prandtl's classical criterion that separation starts at zero wall shear $\tau_x = 0$ was derived for two-dimensional flow, [11]. The present paper, however, deals with three-dimensional flows, and in addition the spanwise scales are small rather than finite in our flows. Some authors have suggested using $n_x \tau_x + n_z \tau_z$, with x, z the wall plane and n_x, n_z the unit vector normal to the separation line as the criterion for separation in three-dimensional flow. (This would presumably become $\tau_x = 0$ at the first point of separation.) One other suggestion we received is that we should instead expect a separation due to the spanwise flow of the type whose asymptotic behavior was described by Stewartson and Simpson [14]. (Actually, this separation *does* have zero wall shear in boundary layer approximation. However, for the similar Banks and Zaturska [15] type of separation process, which might be expected to occur in steady flow for say a wall jet inside a curved pipe, the streamwise wall shear could be anything. That was shown numerically by Van Dommelen [16].)

However, in Appendix B, we provide numerical results that suggest quite strongly that separation does *not* occur at the first wall point with streamwise wall shear zero. We do not use zero wall shear, in any direction, as a criterion for separation. Instead, we have long adhered to the view first explicitly expressed by Sears and Telionis [17]. Since this view is not that well known, we will give a review here.

Already in his pioneering study in 1904, Prandtl [11] had identified zero wall shear as the criterion of steady separation from a fixed wall. This criterion subsequently became widely established as a convenient definition of separation in general. However, in the 1950s, a number of authors, including Moore [18], Rott [19], and Sears [20], (MRS), had expressed concerns about the physical meaning of the criterion in unsteady flows, and in steady flows over moving walls.

Generalizing the earlier work by Moore [18], Sears' Ph.D. student Telionis revisited the question in the 1970s. Based on a study that some called more philosophical than mathematical, Sears and Telionis [17] proposed a generalization of Prandtl's criterion: the separation point would still be at zero wall shear, but not necessarily at the wall. They proposed that in general, the separation point would move with the local flow velocity. This reduces to Prandtl's original condition for steady separation from a fixed wall: in steady flow a separation point cannot move and it is the fluid at the wall that is at rest. Sears & Telionis dubbed the generalized conditions the MRS conditions.

The theory received some support when various early boundary layer computations of relevant flows showed the MRS conditions to apply, [21]. However, these early solutions were subject to the criticism that the prescribed external flow was inconsistent with a separated flow. And there was more criticism. For one, some argued that Prandtl's criterion of zero wall shear remained "convenient" even if the separation was unsteady. More significantly, it was noted that the MRS conditions are incomplete. To apply the MRS conditions to find the separation point requires knowledge of the velocity of the separation point. Now in steady flows that velocity is zero, and in flows with symmetries, like semi-similar flow, it can be deduced from the symmetry. But in general unsteady flows, it requires a priori knowledge of the position of the separation point versus time, the very thing that was to be found.

But Sears & Telionis had an answer to all these criticisms. In 1948, Goldstein [22] had addressed issues in previous numerical work, that computed boundary layers at Prandtl's point of zero wall shear. He showed that at such a point a self-consistent *singular* solution exists, in good agreement with earlier computations by Hartree. Noting this Goldstein singularity, Moore [18] wrote "Of course, the full Navier–Stokes equations do not show such a singularity. However, the existence of *a* singular boundary-layer solution is no doubt a reliable indication of separation, insofar as the boundary-layer equations are able to describe it." (Emphasis added.) Sears and Telionis [17] inverted that: "[…] that the appearance of the Goldstein singularity, *modified as necessary*, in the solution of the boundary layer equations, be adopted as the most general *definition* of separation". (Emphasis added.)

This proposal came under much greater criticism still than the MRS conditions, and from two groups. The first group argued that the Navier–Stokes equations do not have a singularity, and that the interest was in the solution of the Navier–Stokes equations, not the boundary-layer equations. However, this criticism does not allow for much meaningful mathematical analysis in fluid mechanics. As a simple example, consider the case of the thin Blasius' boundary layer along a flush flat plate at large Reynolds number, [23]. Taken literally, that case is nonsensical: mathematics knows no subjective terms like "thin" and "large". Instead it has *limit processes*. In such a setting, "thin" really means that the limit is zero, and "large" that the limit is infinite. Limit processes *require* that the problems are embedded in a larger setting than just a single example flow.

In particular, the limit process relevant for flows like those in this paper is where the Reynolds number is allowed to go to infinity. And that almost unavoidably brings in singularities. The Blasius boundary layer above is rigorously defined as the "jump in flow velocity at the wall at infinite Reynolds number", a singularity. The Blasius velocity profile is rigorously defined as "the limiting flow velocity in suitably rescaled coordinates for infinite Reynolds number", which is nonsingular in this case.

The second group that strongly criticized the singularity proposal consisted of theoreticians. They were familiar with the central role of singularities in any meaningful analysis of fluid flows.

However, they argued that the Goldstein singularity was *the wrong one*. Stewartson [24] had tried to build up a valid *complete* asymptotic separated flow field, one in which the Goldstein singularity provided the upstream end of the separated region. He failed, and his analysis indicated quite strongly that it was not possible. (Subsequently it was found that the Goldstein singularity does occur physically in some other flows not analyzed by Stewartson, [25]. But these flows do not apply to the present study.)

The correct asymptotic flow field corresponding to Prandtl's classical conditions of steady separation from a fixed wall was subsequently identified by Sychev [26] and Smith [27]. It has an upstream singularity much weaker than the Goldstein singularity, one without an intuitive indication that a separation is imminent. (To be fair, neither Moore nor Sears & Telionis suggested that an unmodified Goldstein singularity would appear. Also, if following the ideas Sears & Telionis, a boundary layer computation is conducted using the Sychev–Smith external flow at given finite Reynolds numbers, the resulting position of the Goldstein singularity should give an asymptotically correct location of separation.)

The more important issue was for unsteady flows. The classical example was Prandtl's circular cylinder impulsively started in motion in a direction normal to its axis. This case too was analyzed by Blasius, [23], and he found that after about a third diameter motion, points of zero wall shear develop. But here the very problems appear about which Moore, Root, and Sears were concerned. At least they do if you take the expanded view of a theoretician in which the flow at any Reynolds number is considered. For the steady Sychev–Smith flow above, the boundary layer immediately upstream of the zero wall shear point is vanishingly thin, of order $O(Re)^{-1/2}$. However, immediately downstream the thickness is finite. So there is a solid mathematical justification for saying the boundary layer "separates from the wall" at zero wall shear. The ratio of the boundary layer thickness immediately downstream of zero wall shear to the one immediately upstream of it is unbounded. It becomes *arbitrarily* large when you take the Reynolds number large enough. (Note that this statement does not require a subjective choice of what number is "large".)

The same does *not* happen in case of the impulsively started cylinder after, say, half a diameter motion. The boundary layer at a point downstream of the point of zero wall shear is a bit thicker than at a point upstream of it. However, the ratio stays pretty much the same regardless how large you make the Reynolds number. In the limit of infinite Reynolds number, the boundary layer everywhere collapses at the same rate to an infinite thin one at the surface of the cylinder. Therefore most theoreticians would see very little justification for calling this flow "separated". (At least not in Prandtl's [11] original sense of a significant departure of the boundary layer from the wall, causing a complete change of the flow field.)

(The numerical results in Appendix B suggest, but do not prove, that zero wall shear also fails in the same sense for the Görtler-scale flows studied here.)

The key question was now if the boundary layer solution for the impulsively started circular cylinder would show a singularity at all. (Note that the impulsively started case does not have the problems with the external flow being inappropriate that invalidate the Goldstein singularity in the steady case.) If there was no singularity for any finite time, it might not strictly invalidate the theory of Sears & Telionis, but it would seem to make it fairly academic. And whether there was such a singularity was a matter of considerable controversy, with claims and counter-claims flying about.

Van Dommelen and Shen [28] were the first to provide a numerical solution that showed that a singularity does indeed form, and that could be independently verified. Cowley [29] independently reached an equivalent conclusion using a very different approach. After about 3/4 diameter motion, the boundary layer solution

develops singularities 111° from the front stagnation point, locally terminating the existence of the $O(Re^{-1/2})$ thin boundary layer. This was obviously a considerable victory for Sears & Telionis, especially since the MRS conditions were found to apply. The physical flow development was analyzed in Lagrangian coordinates in [30], and in Eulerian coordinates in [31, Appendix F] and [32]. These studies showed that physically the upper part of the boundary layer is ejected upward away from the wall, like in the Goldstein and Sychev–Smith cases. This flow development leads to a singularity at truly infinite Reynolds number, (or to the used boundary-layer approximation eventually becoming invalid just before that at large Reynolds numbers). But for the Goldstein and the Sychev–Smith singularities, the region near zero wall shear that causes the separation is viscous and thin compared to the upstream boundary layer. For the Van Dommelen & Shen case, the region is inviscid and thick compared to the upstream boundary layer. So, once again the actual singularity bore little resemblance to the Goldstein one.

The other main success for Sears & Telionis was for an already fully developed separation that is in upstream motion compared to the wall. The local asymptotic flow was first described Vic.V. Sychev, with some modifications by later authors [32–34]. This flow too satisfies the MRS conditions. It is inviscid and relatively thick like the Van Dommelen & Shen one. The external flow is of course a fully separated one in this case.

The case of steady separation from a moving wall can be viewed as a simplified case of unsteady separation: the flow seems unsteady when moving along with the wall, (e.g. [17,18]). Therefore such flows have received considerable attention. The Vic.V. Sychev theory above should normally apply to them at high enough Reynolds number. Complete flow fields, at finite Reynolds numbers, for such flows do tend to indicate that the MRS conditions are useful, (e.g. [35–38]). However, as the same references indicate, the Moore–Rott–Sears conditions have not been convincingly verified when the separation point moves downstream compared of the wall.

Various other separation criteria have been proposed over the years for finite Reynolds number flows to generalize zero wall shear. But if these criteria fail for the high-Reynolds-number laminar-flow cases where the physical separation process is well understood, it raises questions about their general value. Despite the difficulty of realizing high-Reynolds-number laminar flows experimentally, theoretically these are the flows where both the governing equations and their solution are most confidently known, (typically using the method of matched asymptotic expansions).

Based on the above background, in this study we judge whether or not an unseparated flow exists by examining whether a *nonsingular* boundary layer flow solution exists everywhere for the assumed attached external flow. If such a solution exists, then there is a self-consistent composite asymptotic flow field in the limit of infinite Reynolds number in which the external flow is attached in a meaningful sense, with viscous effects restricted to a vanishingly-thin, $O(Re^{-1/2})$, boundary layer at the wall. Such a flow clearly would not meet Prandtl's definition of separation.

The problems and uncertainties in trying to formulate a separation criterion are avoided by directly examining whether or not a nonsingular $O(Re^{-1/2})$ thick boundary exists everywhere. But this requires some care. As Sears and Telionis [17] noted, singularity is often associated with obvious numerical problems such as lack of iterative convergence. But obtaining a numerical solution that appears to be smooth is not sufficient to establish nonsingularity; numerical dissipation might smooth singular behavior. It must be shown that the numerical solution converges to a smooth one with mesh size. To do so, the present results were computed at three mesh sizes, representing a factor 4 in mesh size change, corresponding to a factor 16 reduction in estimated numerical error.

For the flows considered here, in the purely two-dimensional case the only type of singularity known to occur is the Goldstein

one, or more accurately the Goldstein–Stewartson one, [22,39,40]. As already mentioned this singularity occurs at zero wall, and it does not occur *physically* for the flows considered. However, our concern is with the *absence* of the singularity. If we encounter the singularity, we simply conclude that the assumed attached flow does not exist. Then we do not care that what we did compute is physically meaningless.

That is also the reason that classical viscous–inviscid interaction is not of interest for the present study, except for the theoretical result of [24]. Here the objective is to establish that an *unseparated* flow field is being created by blowing. It is not to describe the *separated* flow if such an unseparated flow field does not exist. In particular, in the current study only the absence of singularity needs to be established.

When the present flows are not two-dimensional, it is not clear what type of singularity to expect if no attached flow exists. Appendix B summarizes our best numerical observations. However, in the considerable number of Görtler-scale flows of the type considered here that we have computed over the years, we have never seen evidence of singular behavior indicative of separation when the streamwise wall shear remained well clear of zero. Note further that at the first reversal point of the streamwise shear, downstream marching of the boundary layer solution becomes improperly posed. Downstream boundary conditions would be needed to solve the boundary layer beyond that point. For these reasons, the streamwise wall shear remains an important variable. Positive values are an indication, though not a proof, of an "unseparated", i.e. nonsingular, solution.

It may be noted that the three-dimensional Stewartson and Simpson [14] and Banks and Zaturska [15] type singularities are not consistent with the present flows, which include spanwise diffusion. Nor do we consider some straightforward generalization of them very likely to form. We would normally expect diffusive terms to smooth singular behavior. Indeed, for constant streamwise velocity our cross flow satisfies the equivalent of the unsteady two-dimensional Navier–Stokes equations, Section 5. These equations are known to be nonsingular for all time. Thus the streamwise flow must at least be a factor in any singular behavior. And one consequence of the fact that the streamwise flow becomes zero at the wall is that it gives the cross flow diffusion more time to act. Note also that in the two-dimensional Goldstein singularity, the leading order nontrivial term is nonsingular in the transverse direction, though it is singular in the streamwise direction. Consistent with these conjectures, while the computations of Section 6 show some suggestion of spanwise particle motion on a collisional path, this development is arrested before it can develop into a singularity.

3. Effect of two- and normal three-dimensional blowing

The purpose of this section is to give a more objective argument than just practical experience that blowing in incompressible steady two-dimensional boundary layers along fixed walls cannot remove separation. An immediate consequence will then be that three-dimensional blowing cannot remove separation either, as long as the normal three-dimensional boundary layer equations apply. The reason is that these equations do not allow for spanwise interaction except through convection. Therefore their solution at each spanwise position remains quasi-two-dimensional even when the spanwise variations in blowing are finite. So the two-dimensional Goldstein singularity [22,39,40] will still appear at any position of zero (streamwise) shear, and then the analysis of Stewartson [24] still indicates that the assumed attached flow does not actually exist.

This section will accept as an empirical numerical observation that a two-dimensional steady laminar boundary layer over a fixed wall with a given attached external flow terminates in a Goldstein singularity when the wall shear becomes zero. Over the years, numerous numerical computations, including ones by the first author, [12,13], have shown that the Goldstein singularity appears at zero wall shear with or without blowing.

It will further be assumed that in the presence of the Goldstein singularity, there is no longer a composite asymptotic flow field consisting of an attached external potential flow and a thin boundary layer near the wall, [24]. Without an asymptotic flow field in which the external potential flow is the attached one, the flow is physically separated in the sense discussed in the previous section.

It should be noted that there are some limitations to the above assumptions, as discussed more fully in Appendix B. Most prominently, in the marginal case that the wall shear becomes zero at a single point, with the shear still positive upstream and downstream of the point, the Goldstein singularity takes a degenerate form. In that case, the flow is still unseparated in the sense of Section 2.

Now consider the precise question to be addressed in this section. Suppose that for a given (attached, two-dimensional) external flow, the boundary layer solution ends in a point of zero wall shear. The Goldstein singularity at such a point implies that the assumed attached flow does not exist. The real flow must be separated. The question is whether blowing through the wall might be able to increase the wall shear above zero everywhere, thus allowing the desired attached flow to be achieved. It will be shown that the answer is no; blowing will invariably reduce the wall shear. Therefore, it can only generate a separated flow where none existed before.

It may first be mentioned that there are various rigorous results about the absence of separation in a strictly favorable pressure gradient, and about the shape of the velocity profile, [41,42]. (Unfortunately the latter more accessible reference omits the blowing velocity.) Oleînik and Samokhin [43] give an extensive review of what has been proved rigorously for the boundary layer equations.

The relevant two-dimensional momentum and continuity equations and wall boundary conditions are, in suitable scalings, [44],

$$uu_{,x} + vu_{,y} = -p_{,x} + \tau_{,y} \quad u_{,x} + v_{,y} = 0$$
$$\tau \equiv u_{,y} \quad [u = 0]_{\text{wall}} \quad [v = v_{\text{w}}(x)]_{\text{wall}}. \tag{1}$$

Here x is the nondimensional distance along the wall and y the scaled nondimensional distance away from it; u and v are the corresponding velocity components; $p(x)$ is the given pressure (corresponding to unseparated flow); $v_{\text{w}}(x)$ the given blowing velocity; and τ the scaled nondimensional shear (or negative vorticity). Subscripts following a comma indicate partial derivatives.

To examine the effect of the blowing, the above problem will be embedded in a generalized one. The generalized problem differs from the one above in that the wall blowing velocity is some multiple t of the given blowing velocity v_{w}, with $0 \le t \le 1$ a parameter. So $t = 0$ gives the solution without blowing, while $t = 1$ gives the solution for the given blowing velocity. When t is gradually increased from 0 to 1, the solution changes from the one without blowing to the one with the given blowing velocity. (One may take the parameter t to be time in a quasi-steady process in which the blowing distribution is gradually increased from zero.)

It will be assumed that the solution of the generalized problem is a smooth function of both the spatial coordinates and the parameter t as long as τ stays above zero. The only singularities observed numerically are at zero shear, (cf. [45, p. 371]). For a strictly favorable pressure gradient, it has in fact been shown rigorously that a well-behaved solution exists for the standard boundary layer problem, [42,43].

Using the assumptions above and asymptotic expansion procedures, it will be shown that the derivative τ' of the shear with respect to t is never positive. Therefore, the shear will go down, rather than up when the blowing is applied between $t = 0$ and $t = 1$. Therefore, the shear cannot be increased above zero and so the separation cannot be removed.

Since the shear τ is the critical quantity, it is convenient to make it the dependent variable. That can be done by taking a y derivative of the momentum equation above and applying the continuity equation. It is further convenient to take u as an independent variable instead of y. That gives the Crocco [46] equation:

$$u\tau_{,x} - p_{,x}\tau_{,u} = \tau^2 \tau_{,uu} \quad [v = tv_{\text{w}}]_{\text{wall}} \quad [v\tau = -p_{,x} + \tau \tau_{,u}]_{\text{wall}} . \quad (2)$$

The additional wall boundary condition is the momentum equation at the wall $u = 0$.

Differentiation with respect to t gives

$$u\tau'_{,x} - p_{,x}\tau'_{,u} = \tau^2 \tau'_{,uu} + 2\tau \tau_{,uu}\tau' \quad \left[\tau \tau'_{,u} + \frac{p_{,x}}{\tau}\tau' = \tau v_{\text{w}}\right]_{\text{wall}} \quad (3)$$

where a prime denotes a partial t derivative.

The above is a linear equation for τ' given the flow at any value of t. The solution for τ' can be written as

$$\tau'(x, u) = \int_{\text{all } x_0} v_{\text{w}}(x_0)G(x, u; x_0) \, dx_0 \quad (4)$$

where $G(x, u; x_0)$ is the response at position x, u to a delta function blowing velocity at x_0. The values of x_0 range over the chosen blowing distribution. Note however that $G(x, u; x_0)$ is zero for $x < x_0$, since the boundary layer equation has no upstream influence.

To prove the desired result that the blowing v_{w} cannot remove the separation, it suffices to show that $G(x, u; x_0)$ is everywhere nonpositive. That implies the needed result above that τ' is positive, because then the integrand in (4) is.

(Note that the result will be somewhat stronger than merely that the total blowing distribution cannot remove separation. It will imply that every separate infinitesimal part of the blowing distribution can only decrease the shear. So no part of the blowing distribution can have a beneficial effect on separation.)

First note that $G(x, u; x_0)$ is a solution of Eq. (3) for τ' when v_{w} is a delta function at x_0. Since in the equation, τ is an arbitrary nonconstant function, there is no simple solution even for a delta function blowing velocity. In lack of such a solution, we will use a two-part argument. First an argument will be given to show that if solutions τ' to (3) are initially nonpositive, and negative at the wall, they will stay nonpositive for all x. Then we will use an asymptotic expansion for $x \rightarrow x_0$ to argue that solution $G(x, u; x_0)$ is indeed initially of that form.

First consider therefore an arbitrary solution τ' to (3) that at some initial x is negative at the wall, and nonpositive elsewhere. Also assume for now that the corresponding v_{w} is positive beyond the initial x. Under those conditions, consider the possibility of τ' developing positive values at any arbitrary downstream point before the terminating Goldstein singularity. In particular, let τ'_{m} be the hypothetical positive maximum of τ' over all u for given x. Because of the assumed initial condition and nonsingularity, τ'_{m} must have evolved from an initial zero value. This initial zero value cannot be at the wall, because the wall boundary condition in (3) would imply that there are already positive values of τ' above the wall at that point. However, the initial zero value cannot be at a finite distance from the wall either. To see that, divide (3) by $u\tau'$ to get, at the maximum,

$$\frac{d \ln \tau'_{\text{m}}}{dx} = \frac{\tau^2}{u\tau'_{\text{m}}}\tau'_{,uu} + \frac{2}{u}\tau \tau_{,uu}. \quad (5)$$

The left-hand side integrates to positive infinity between the zero point and any existing positive value. However, the first term in the left-hand side is nonpositive at the maximum while the second term is finite. So the two sides cannot match, which implies that the postulated positive maximum cannot develop this way.

Finally the positive τ'_{m} cannot originate from infinity either. This seems intuitively obvious; consider a computation that would use a cut-off at a large value of the stream function ψ. Assume that this computation would prescribe a decreasing fraction of the positive vorticity at the cut-off as estimated from asymptotic analysis. (This

should surely be no worse than prescribing zero vorticity at the cut off.) Then if positive τ' originates from infinity, this computation could not produce it. Then the error in the computation could not go to zero even when the position of the cut off is allowed to become infinite. That is hard to believe.

Mathematically, the fact that indeed positive τ'_{m} cannot originate from infinity can be derived using asymptotic analysis. To do so, Von Mises coordinates will be used, in which the stream function ψ is taken as the independent coordinate instead of u or y. The vorticity and the vorticity equation can then be written as

$$\tau \equiv e^{-Q} \qquad Q_{,x} = -uQ_{,\psi}^2 + uQ_{,\psi\psi} + u_{,\psi}Q_{,\psi}.$$

Assuming that the blow up of Q for infinite ψ takes the asymptotic form of powers of ψ times powers of $\ln \psi$, it is seen that Q must be $O\left(\psi^2\right)$. Otherwise the first term in the right-hand side cannot be matched. Then the critical final term in (5) above,

$$\frac{2}{u}\tau \tau_{,uu} = -2uQ_{,\psi\psi} - 2u_{,\psi}Q_{,\psi}$$

stays finite at infinity. Then according to (5), positive τ' cannot originate from infinity either.

While this argument is based on asymptotic analysis, and therefore not a rigorous proof, there are some rigorous results that support it. In terms of y, (note that $\psi = O(y)$ for large y),

$$u = u_{\text{e}}(x) - e^{-q} \qquad 2\tau \tau_{,uu} = \frac{\partial}{\partial y}\left(\frac{u_{,yy}}{u_{,y}}\right). \quad (6)$$

An asymptotic suction profile has q linear in y, and Theorem 4 of [47] implies that in a further evolution of such a profile, q remains bounded between linear expressions in y. Quadratic blow up of q occurs for profiles that develop from similarity solutions, [47]. In particular Theorem 5 in that reference implies that if the initial condition for q is bounded between quadratics in y, then it remains bounded between such quadratics. The strongest result for the present case may be Theorem 3.3.1 of [43]. It shows that for suitable initial conditions, in which $2\tau \tau_{,uu}$ is initially finite, it stays finite for at least some x-range, or for any x in case of a favorable pressure gradient.

The conclusion is that if τ' is initially nonpositive, and negative at the wall, it cannot become positive as long as the blowing velocity is positive. This result can be strengthened slightly: the blowing velocity can be allowed to be zero. The reason is that zero blowing velocity is the limit of positive blowing velocity. Assuming properly-posedness, the limit of nonpositive τ' cannot be positive.

Therefore if $G(x, u; x_0)$ is initially nonpositive, and negative at the wall, it will stay nonpositive for all x. To show that $G(x, u; x_0)$ meets these requirements, asymptotic analysis will again be used. Consider first the response of Eq. (3) to a blowing distribution v_{w} given by a Heaviside unit step function at a position x_0. Upstream of x_0, the solution τ'_{H} will be zero since the boundary layer equation has no upstream influence. Downstream of x_0, asymptotic analysis shows that the solution for $x \rightarrow x_0$ takes the same form as that immediately behind a jump in wall blowing in the usual boundary layer equations:

$$\tau'_{\text{H}} \sim -\tau_0^{2/3}\bar{\xi}^{1/3}f(\bar{\eta}) \qquad \bar{\xi} \equiv x - x_0 \downarrow 0 \qquad \bar{\eta} \equiv \frac{u}{\tau_0^{2/3}\bar{\xi}^{1/3}}. \quad (7)$$

Here τ_0 is the wall shear at x_0. The above solution can be found in [12] with function

$$f(\bar{\eta}) = \left[3e^{-\bar{\eta}^3/9} - \bar{\eta}\int_{\bar{\eta}}^{\infty}\bar{\eta}_0 e^{-\bar{\eta}_0^3/9}\,d\bar{\eta}_0\right] \Bigg/ \int_0^{\infty}\bar{\eta}_0 e^{-\bar{\eta}_0^3/9}\,d\bar{\eta}_0 \quad (8)$$

given in terms of the incomplete Gamma function, but an equivalent solution in terms of hypergeometric functions can be distilled from [48]. It is also implicit in the linearized interactive solution of [49] after scaling away the interaction region. While this is an asymptotic solution, and therefore not rigorous, (as is the Goldstein–Stewartson singularity, for that matter), its applicability to

the normal boundary layer equations has been verified numerically, [12].

The response to a delta function blowing velocity can be obtained by taking the limit for $\varepsilon \downarrow 0$ of the sum of an upward step of height $1/\varepsilon$ at x_0 and an opposite downward step at $x_0+\varepsilon$. That gives

$$G(x, u; x_0) \sim -\tau_0^{2/3} e^{-\bar{\eta}^3/9} / \bar{\xi}^{2/3} \int_0^\infty \bar{\eta}_0 e^{-\bar{\eta}_0^3/9} \, d\bar{\eta}_0$$

$$\bar{\eta} \equiv \frac{u}{\tau_0^{2/3} \bar{\xi}^{1/3}}. \tag{9}$$

This is the exact response for the leading order equation

$$u\tau_{,x}' = \tau_0^2 \tau_{,uu}'$$

to a delta function Neumann boundary condition. (That it is a solution is readily verified by direct substitution. The coefficient can be verified by integrating the above equation over a semi-infinite vertical strip.) Therefore it is an asymptotic solution of the original equation for finite $\bar{\eta}$. Note further that the integral can be written in terms of $\Gamma(\frac{2}{3})$.

(It might seem conceivable that there could be some, so far unrecognized, nontrivial expansion intermediate to the $\bar{\eta}$ and finite u ones in which G could reverse sign. However, this turns out not to be possible on behalf of (5) since u would exceed $O(\bar{\xi}^{1/3})$.)

4. Governing equations for Görtler-scale blowing

The previous section showed that according to the usual three-dimensional boundary layer equations, transverse blowing cannot remove separation in an originally two-dimensional boundary layer. In particular, transverse blowing invariably decreases the streamwise wall shear rather than increases it. However, the experiments show that removal of separation is possible. Therefore, it seems logical to look for assumptions in the normal boundary layer that may need to be modified to explain the experiments qualitatively.

Looking at the experiments, the most obviously suspect assumption is that the spanwise scales are finite. In the experiments, the microjets are a fraction of a millimeter in diameter, and their spanwise spacing is comparable to the thickness of the turbulent boundary layer. For laminar boundary layers along slightly curved walls, it is well known that spanwise convection and diffusion are no longer negligible on a spanwise scale of the order of the boundary layer thickness. These Görtler scalings have been studied extensively in the framework of boundary layer instabilities, [50,51].

In the present study, it will be assumed that the flow is periodic in the spanwise direction, with a period of order of the boundary layer thickness. The arc length along the wall, measured from the start of the boundary layer, will be denoted by $\tilde{x}$, the transverse distance from the wall as $\tilde{y}$, and the spanwise coordinate as $\tilde{z}$, with period $\tilde{\lambda}$. The corresponding velocity components are $\tilde{u}$, $\tilde{v}$, and $\tilde{w}$; the pressure is $\tilde{p}$; the constant density is $\tilde{\rho}$; and the wall curvature is $\tilde{\kappa}$. To prevent centrifugal acceleration from fully dominating the cross-plane pressure field, the wall curvature needs to be asymptotically small. Using a suitable reference velocity $\mathcal{U}$ and reference length ℓ, the following scaled nondimensional variables can be defined inside the boundary layer:

$$x = \frac{\tilde{x}}{\ell} \qquad y = \frac{\tilde{y}}{\ell}\sqrt{Re} \qquad z = \frac{\tilde{z}}{\ell}\sqrt{Re}$$

$$u = \frac{\tilde{u}}{\mathcal{U}} \qquad v = \frac{\tilde{v}}{\mathcal{U}}\sqrt{Re} \qquad w = \frac{\tilde{w}}{\mathcal{U}}\sqrt{Re} \tag{10}$$

$$p = \frac{\tilde{p} - \tilde{p}_a}{\tilde{\rho}\,\mathcal{U}^2} Re \qquad \lambda = \frac{\tilde{\lambda}}{\ell}\sqrt{Re} \qquad \kappa = \tilde{\kappa}\ell\sqrt{Re}$$

where $\tilde{p}_a$ is the spanwise-averaged wall pressure and $Re = \mathcal{U}\ell/\tilde{\nu}$ is the Reynolds number.

Substitution into the Navier–Stokes equations, written in boundary layer coordinates, yields the following asymptotic equations:

$$uu_{,x} + vu_{,y} + wu_{,z} = u_{,yy} + u_{,zz} + u_e u_{e,x} \tag{11}$$

$$uv_{,x} + vv_{,y} + wv_{,z} = v_{,yy} + v_{,zz} - p_{,y} + \kappa u^2 \tag{12}$$

$$uw_{,x} + vw_{,y} + ww_{,z} = w_{,yy} + w_{,zz} - p_{,z} \tag{13}$$

$$u_{,x} + v_{,y} + w_{,z} = 0. \tag{14}$$

These equations are known in numerical work as the "fully parabolized Navier–Stokes equations". Compared to the full Navier–Stokes equations, there is neither a streamwise pressure interaction nor a viscous diffusion term to bring in dependence on the downstream solution. As asymptotic equations for high Reynolds numbers, and including curvature, they are attributed to Hall [52].

It will be assumed that the flow above the boundary layer is a potential flow. In this potential flow all spanwise variations decay exponentially within a distance of the order of the period. Therefore, at physically finite distances above the boundary layer, the flow will be two-dimensional. However, there may be a small constant spanwise velocity component that persists. Flow quantities immediately above the boundary layer will be indicated by a subscript e. Matching requires:

$$u \sim u_e \qquad v \sim -u_{e,x}y + v_d \qquad w \sim w_e$$

$$p \sim \frac{1}{2}\left(u_e u_{e,xx} - u_{e,x}^2\right)y^2 + \left(u_{e,x}v_d - u_e v_{d,x} + \kappa u_e^2\right)y + p_{e0} \tag{15}$$

where the remainders are exponentially small and u_e, v_d, and p_{e0} are functions of x, while w_e is constant. All computations reported here take w_e to be zero.

The wall boundary conditions in this study are

$$u = w = 0, \quad v = v_w(x, z), \quad \text{at } y = 0 \tag{16}$$

where v_w is a chosen blowing distribution. The boundary conditions at infinity are

$$u \sim u_e(x), \quad w \sim 0, \quad \text{for } y \to \infty \tag{17}$$

where u_e is a chosen external flow. Periodic boundary conditions are used in z, the scaled period being λ.

In the limit in which λ tends to infinity, u and v become quasi-two-dimensional. However, the scaled spanwise velocity w does not become zero. There is an interaction between the viscous boundary layer flow and an inviscid upper deck above it that maintains a nonzero spanwise velocity component.

5. Numerical scheme

According to the previous section the asymptotic Görtler-scale blowing problem requires solution of the parabolized Navier–Stokes equations (11)–(14). These equations must be solved numerically. Suitable numerical schemes are more complex than for the normal three-dimensional boundary layer equations. The additional problems are the spanwise diffusion terms and especially the fact that the cross-flow pressure gradients are unknown.

The computations here are based on the use of the physical velocity and pressure variables. In that respect they are similar to the ones of [53], who used a SIMPLE algorithm. Many other existing schemes tend to be inspired by and/or targeted for stability problems, [52,54,55].

Note that if the streamwise velocity is everywhere equal to a constant, the Eqs. (11)–(14) are identical to the two-dimensional unsteady Navier–Stokes equations (with x/u as "time"). Unfortunately, the streamwise velocity is not constant but drops to zero at the wall. That makes the effective "time" step near the wall very

large. In particular, the Courant number near the wall blows up with mesh refinement, assuming it is at an equal rate in all three directions.

There are additional complications due to the fact that an asymptotic problem is solved. It means that the distance away from the wall extends to infinity. Furthermore the velocity in that direction and the pressure become infinite with distance away from the wall.

In addition, for a flat-plate-like boundary layer as computed here, one that starts at zero thickness and continues to downstream infinity, there is a problem of vastly unequal scales. At the start of the boundary layer, the boundary layer thickness is much smaller than the spanwise period. Far downstream it is the other way around. (Physically, at the start of the boundary layer there is a thin viscous layer with an inviscid upper deck above it. Far downstream, there is a three-dimensional layer at the wall with a thick two-dimensional boundary layer above it.) In the transverse direction, sufficient mesh points must be provided to resolve the flow on both scales.

To deal with these challenges, the code uses algebraic mappings of the x, y, z flow domain onto a unit cube in a computational α, β, γ domain. Modified dependent variables were defined to account for the infinities. Details can be found in Appendix A.

A final problem is a bit less self-evident. The thin boundary layer at the start of the plate contains highly concentrated streamwise vorticity. (Velocity component w blows up proportional to $x^{-1/2}$ at the start of the boundary layer, the same as v, generalizing the behavior of Blasius flow. But in addition the viscous y-range is small of order $x^{1/2}$.) In a numerical computation it may be hard to describe the strong exponential decay of the vorticity at the upper edge of the viscous layer accurately. The length scale of the decay becomes smaller with distance from the wall while the mesh spacing is expanding to accommodate the much thicker upper deck. So some vorticity might "leak out" somewhat into the overlying potential flow due to numerical errors. That concentrated vorticity will drift downstream in the potential flow until it hits the boundary layer at a station where the vorticity levels are much lower. So even a small amount of vorticity, on the upstream scale, may provide a significant error at a downstream station. Consistent with this idea, we encountered convergence problems in the initial region when the computation started out fully three-dimensional. The only solution we found to work was to use a cut-off at a suitable large value of y above which we prescribed a zero vorticity condition instead of z-momentum.

Of course, the cut-off adds an additional parameter to worry about. Every numerical solution produced a plot of the value of the streamwise velocity and vorticity at the cut-off, to ensure that the vorticity at it was accurately zero. In addition, every flow was computed for at least two values of the cut-off, to ensure that the results are independent of its location. Fortunately, the vorticity decays exponentially with distance from the wall, and it was generally observed that the cut-off did not produce a perceivable difference in the results as long as it was sufficiently clear of the vorticity layer but not far enough for the mesh nonlinearity to become a major factor.

The finite difference equations in each cross plane were solved iteratively using a custom scheme. It is based on the p' method of [56]. The p' method is relatively intuitive, simplifying its adaptations to handle the infinitely thin viscous layer thickness at the start of the computation and the infinite mesh spacing at infinity. The custom scheme appears to be "fast" in the sense that the computational time per mesh point is approximately independent of mesh size. Since this is described in [57], the details can be skipped here. As long as the equations are fully converged, the iterative scheme does not make a difference. All results presented here are fully converged, to a target maximum error of no more than 10^{-8}.

Note that this is the actual truncation error in the relevant transformed equations, not a difference between iterates, and not multiplied by a small mesh size. In various computations at the finest meshes 10^{-8} seemed to be more than round-off error allowed, and the maximum value was then allowed to increase to 10^{-7}. (It may seem surprising that a 10^{-8} error would not be achievable in 64 bit precision for the meshes used. However, these problems typically occurred relatively far downstream, where the period-scale mesh spacing is much smaller than the viscous-scale one.)

All computations were conducted at 3 mesh sizes, with each mesh size a factor two larger in each direction than the previous one. This corresponds to a factor 16 reduction in numerical error from the coarsest mesh to the finest. Convergence analysis based on these results indicates that the results presented in the next sections are everywhere accurate to at least about line thickness, Appendix A.

6. Removal of marginal separation by blowing

The objective in this section is to show that Görtler-scale blowing can indeed remove separation under at least some circumstances. This will prove that the restrictions of Section 3 do not apply to those flows.

To show this, first a suitable external flow must be chosen. Note that any desired external flow can always be achieved by suitable shrouding, for example by creating a slender duct. For the present purposes, a marginally separated two-dimensional flow provides a convenient example. For a separation that is much stronger than marginal, removal of separation by blowing might be difficult or impossible within the current framework. Even if it is not, the stronger required blowing would put very high demands on numerical accuracy. In addition, for a marginal separation the boundary layer both upstream and downstream of the marginal separation location is known. The solution with blowing can be compared with it to assess the various effects of the blowing.

There are some other desirable characteristics for the marginally separated flow. To avoid having to choose arbitrary initial conditions, it is desirable to start the boundary layer as a three-dimensional generalization of a similarity solution. In particular, the boundary layer was assumed to start at finite velocity and zero thickness like the Blasius boundary layer in two-dimensions. (A Hiemenz-like initial condition would be another logical choice. However, the initial condition would be more difficult to obtain due to the finite boundary-layer thickness.)

Such an initial condition has the further advantage that the initial flow can be compared to theoretical results obtained by asymptotic expansions. That provides a check on the numerical solution, but more importantly, it allows the initial flow to be well understood theoretically.

Note that a Blasius-type assumption of a boundary layer that starts at zero thickness brings in a corresponding singularity at the initial position. It has been suggested that it would be better to provide some modified initial condition that avoids the singularity. We must disagree, and not just for the reasons mentioned above. The further reasons are the same as those for which fluid dynamicists will still study the flat plate as a fundamental example, and not say some thin paraboloid or ellipsoid that would avoid the Blasius singularity. Not only does an artificial "smoothing" of the singularity increase the parameter space by an additional dimension, the appropriate smoothing parameter to still approximate a flat plate also brings in a Reynolds number dependence. That eliminates the great advantage of boundary layer theory of providing a solution that is asymptotically independent of the Reynolds number.

It is also convenient to assume that far downstream, the external flow velocity is again constant. This is to ensure that the separation is eliminated, and not merely pushed downstream. When the

flow is seen to return to a Blasius boundary layer, it can reasonably be concluded that no separation will occur farther downstream.

A suitable external flow meeting these constraints can be obtained using the approximate Pohlhausen method and some heuristic considerations, Appendix C. The external flow, and the corresponding two-dimensional wall shear without blowing, are shown in Fig. 1. The velocity drops monotonously a total of 36% going downstream. Marginal separation is found to occur at a normalized streamwise coordinate $x = 2.93$.

Despite considerable numerical experimentation, so far we have been unsuccessful in removing separation assuming that the wall is flat. Our general observation in these computations is that blowing initially has an unfavorable effect on separation. While Görtler-scale streamwise vortices are created, they do not seem to be sufficient to offset the initial unfavorable effects. If the scaled spanwise period λ is small, the vortices diffuse away quite rapidly. For larger scaled periods, the vortices are too far apart to prevent separation between them.

However, the Stratford ramp flow [2–4] has a concave wall in the region of separation. Since in Görtler scalings, any wall curvature is asymptotically small, even a small amount of curvature can correspond to a large scaled curvature. This can strengthen the streamwise vorticity following the Görtler mechanism, [52].

In the example presented in this section, it allows the vortices to survive long enough to remove the marginal separation. In this example, the curvature was taken to be

$$\widehat{\kappa}_0 \equiv \widetilde{\kappa}\widetilde{x}\sqrt{\frac{\widetilde{u}_e(0)\widetilde{x}}{\widetilde{\nu}}} = -10. \tag{18}$$

Here $\widetilde{u}_e(0)$ is the external flow velocity at the start of the plate.

The corresponding wall blowing velocity was taken to be

$$\begin{aligned}
\widehat{v}_{w0} &\equiv \frac{\widetilde{v}_w}{\widetilde{u}_e(0)}\sqrt{\frac{\widetilde{u}_e(0)\widetilde{x}}{\widetilde{\nu}}} \\
&= C_v \tan\left[f_v\frac{\pi}{4}\left(1-\cos\frac{2\pi\widetilde{z}}{\widetilde{\lambda}}\right)\right] e^{-(\xi_0/\ell_v)^2}
\end{aligned} \tag{19}$$

$$C_v = 0.0694 \quad f_v = 0.875 \quad \ell_v = 0.034.$$

The parameter f_v allows a spiky spanwise blowing distribution to be described, to more closely resemble a microjet. In particular, the blowing velocity in the center of the period becomes infinite for $f_v = 1$. For practical purposes, the values of f_v are limited by numerical resolution. Parameter C_v adjusts the strength of the blowing, which must be kept low enough to prevent separation in the initial region. The final exponential describes the streamwise decay of the blowing distribution. It is in terms of the streamwise coordinate
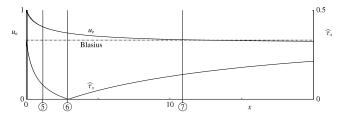
$$\xi_0 \equiv \frac{\widetilde{x}}{\widetilde{\lambda}}\sqrt{\frac{\widetilde{\nu}}{\widetilde{u}_e(0)\widetilde{x}}}. \tag{20}$$

The coordinate ξ_0 is particularly convenient to describe the initial flow, where the boundary layer is thin compared to the period. In particular, ξ_0 arises naturally in the asymptotic equations when written in the Blasius-type similarity variables

$$\eta_0 \equiv \frac{\widetilde{y}}{\widetilde{x}}\sqrt{\frac{\widetilde{u}_e(0)\widetilde{x}}{\widetilde{\nu}}} \quad Z \equiv \frac{\widetilde{z}}{\widetilde{\lambda}}. \tag{21}$$

In the asymptotic equations, $\widetilde{x}$ appears only in the combination ξ_0. Use of ξ_0 instead of x also eliminates the Blasius-type square root singularity in the flow variables at the start of the plate.

Note that the figures will use ξ and η, normalized with the local external flow velocity $\widetilde{u}_e$ instead of $\widetilde{u}_e(0)$, rather than ξ_0 and η_0. We find the constant initial velocity more intuitive in comparing flow parameters. However, the local velocity is more suitable for plotting, especially for the velocity profiles. The plotted dependent

Fig. 1. External flow and the corresponding marginal separation without blowing. Vertical lines refer to plotted stations for the solutions with blowing.

variables are

$$\widehat{u} \equiv \frac{\widetilde{u}}{\widetilde{u}_e} \quad \widehat{\tau}_x = \frac{\widetilde{\tau}_x}{\widetilde{\rho}\,\widetilde{u}_e^2}\sqrt{\frac{\widetilde{u}_e\widetilde{x}}{\widetilde{\nu}}} \quad \widehat{\omega}_x = \widetilde{\omega}_x\frac{\widetilde{x}}{\widetilde{u}_e}$$

$$\widehat{v}_d \equiv \frac{\widetilde{v}_d}{\widetilde{u}_e}\sqrt{\frac{\widetilde{u}_e\widetilde{x}}{\widetilde{\nu}}} \quad \widehat{p} = \frac{\widetilde{p}-\widetilde{p}_a}{\widetilde{\rho}\widetilde{u}_e^2}\frac{\widetilde{x}}{\widetilde{\lambda}}\sqrt{\frac{\widetilde{u}_e\widetilde{x}}{\widetilde{\nu}}} \tag{22}$$

for the streamwise velocity, shear, and vorticity, the displacement velocity, and the cross-plane pressure, respectively. The displacement velocity is the velocity that the boundary layer induces in the potential flow immediately above the boundary layer. It is well known that the displacement thickness is a more awkward quantity in three dimensional flows. (However, for the current flows, the displacement thickness could in principle be found by taking a spanwise average of the two-dimensional expression.)

Figs. 2 and 3 show the numerical results. In particular, Fig. 2(a) shows the streamwise wall shear $\widehat{\tau}_x$ and displacement velocity $\widehat{v}_d$ for the marginally-separated two-dimensional flow in terms of ξ. The various features described by [58–60] are evident.

Fig. 2(b) shows how the three-dimensional blowing raises the wall shear well above zero in the region where the two-dimensional flow would separate. On the other hand, now the minimum shear dips down quite close to zero in the very early development. However, the solution remains nonsingular. Far downstream, the Blasius wall shear is approached, but slowly. At the end of the plotted range, corresponding to $x = 51$, the shear is only 80% of the Blasius value. However, at the end of the computation, corresponding to $x = 102$, that has improved to 91%. It appears therefore that the separation has been fully eliminated, not just pushed downstream.
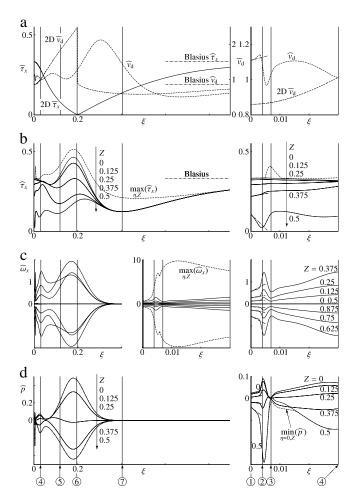
Consider now some physics of the flow. One surprising observation is the existence of two very disparate length scales, as evident in the figures. In fact, we found it convenient to plot the initial development on a different ξ-scale than the later one. The short initial scale is not a numerical artifact. It is fully supported by an asymptotic expansion of the initial flow, shown as straight dot–dash lines. The asymptotic expansion is essentially exact. Note that the asymptotic solution is not used in the finite difference solution of the full problem. The finite difference equations implicitly create their own initial conditions. So the excellent agreement in both the initial values and initial slopes is nontrivial.

The very early development is accurately described by the asymptotic solution. A typical streamwise station is indicated by 1, (encircled), in Figs. 2 and 3. The streamwise velocity profiles at this early stage are shown at the top left in Fig. 3. These are Blasius profiles including a wall blowing velocity. The maximum blowing velocity (19) is 0.35 and occurs at the center of the period. This stays well clear of the value 0.6192472 at which the Blasius profile gets "blown-off", [61–65].

The contour lines of streamwise vorticity at station 1 are plotted below the velocity profiles in Fig. 3. They show two counter-rotating vortices away from the wall above a reversed vorticity layer near the wall. Like the velocity profiles, the finite difference and asymptotic results are identical at this station.

The reason for the reversed vorticity at the wall can be readily understood. In this early stage, the viscous layer is thin enough that the streamwise vorticity is dominated by the $w_{,y}$ term, with w

Fig. 2. Removal of separation by blowing: (a) streamwise wall shear and displacement velocity (2D means no blowing), (b) streamwise wall shear, (c) streamwise vorticity, (d) wall pressure. Mesh size is $1024 \times 192 \times 256$. Solid lines are wall values and dot–dash ones asymptotic theories.
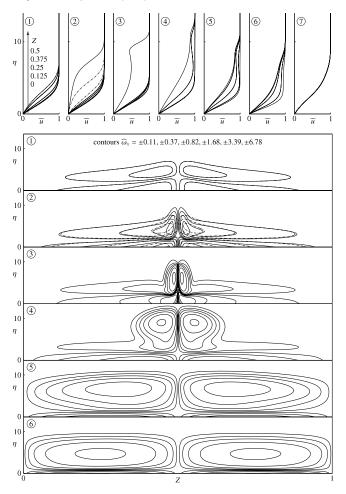

Fig. 3. Top: streamwise velocity profiles. Remainder: streamwise vorticity contours. Encircled numbers indicate the streamwise locations shown in Fig. 2.

the spanwise velocity and y the distance from the wall. The strong blowing near the center of the period creates a displacement effect above the viscous layer that drives a flow away from the symmetry plane. However, the Blasius-type scalings imply that

$$w \propto 1/\sqrt{x}.$$

Physically this corresponds to a deceleration of the potential flow away from the symmetry plane with increasing x. The corresponding spanwise pressure force is directed toward the symmetry plane, cf. Fig. 2(d). This pressure force drives the viscous fluid particles immediately above the wall toward the symmetry plane. Hence a reversal of the sign of $w_{,y}$ must exist in the interior of the viscous layer.

There is a feedback mechanism, as the particle motion near the wall has a compressive effect on the spanwise vorticity at the symmetry plane. That tends to reduce the spanwise vorticity, or equivalently the streamwise wall shear, following Kelvin's theorem. Fig. 2(b) shows that the initial rapid evolution toward separation is well understood from second order asymptotic theory.

However, when station 2 is reached, the first order asymptotic theory is self-evidently no longer a reasonable first approximation. The velocity profiles, Fig. 3, show a dramatic thickening of the boundary layer, as might be expected from the near-separation. Note also that the true velocity profiles are now very different from even the second order asymptotic theory, shown as dot–dash lines. Similarly, the contour lines in Fig. 3 show that the streamwise vortices are quite different, and stronger, than the ones predicted by the asymptotic theory.

Why the trend toward separation gets arrested around station 2 is not obvious. We would ascribe it tentatively to spanwise diffusion. To be sure, at station 2 the boundary layer is still very thin compared to the spanwise scale $\tilde{\lambda}/2\pi$. So normally the spanwise diffusion would be expected to be a minor effect. However, as the velocity profiles and vorticity contours in Fig. 3 indicate, the region of near-separation around the center period is quite sharp. In addition, Lagrangian motion will carry fluid from regions with significantly higher shear closer to the center plane over time. And qualitatively, it is well known that it does not take that much for a laminar boundary layer to separate.

Note however that in addition to the streamwise vorticity, the deceleration of the streamwise motion contributes to the cross plane velocity field. This contribution takes the form of a source distribution that wants to drive the fluid away from the center plane.

The displacement velocity, shown in Fig. 2(a), does not show much evidence of the significant developments in the viscous layer at the center plane. The reason is that the displacement velocity applies to the motion above the inviscid upper deck. The upper deck has a thickness comparable to the period, much more than the thickness of the viscous layer. So only an average of the evolution over the entire period is evident in the displacement velocity.

After recovery, the wall shear quickly returns to a level much more consistent with first order asymptotic theory. However, going from station 2 to station 3, there is some additional thickening of the velocity profiles, Fig. 3. (For station 3 and beyond, the small-x asymptotic results will no longer be shown.)

There are a couple of surprising features of the velocity profiles at station 3. Noting that the streamwise shear is given by the slope

of the velocity profile, it is seen that an internal point of maximum shear has developed that exceeds the values at the wall. This maximum corresponds to the "hump" in the dotted line in Fig. 2(b) that gives the global maximum shear. Secondly, the shear has developed negative values in the interior of the boundary layer.

The relative strengthening of the shear might be readily understood as the opposite of the process that reduced the wall shear at the wall: the streamwise vortices will produce stretching of the spanwise vorticity near the top of the viscous layer. The formation of the reversed shear is more complex. This process would not even be possible in a two-dimensional boundary layer, [41]. Taking the y-derivative of the streamwise momentum equation, the evolution equation for the shear is seen to be

$$\frac{\mathrm{d}\tau_x}{\mathrm{d}x} = \tau_{x,yy} + \tau_{x,zz} + w_{,z}\tau_x - w_{,y}u_{,z}.$$

The left-hand side is the derivative of the shear following the cross-plane particle motion, or following a local extremum in shear. The first two terms in the right-hand side will always reduce the magnitude of an internal extremum of shear. The third term, the vortex stretching effect already mentioned, can increase an extremum. But it cannot reverse the sign of the shear, cf. Section 3. The final term in the right-hand side is zero at the center plane by symmetry. It can be concluded that the reversed shear cannot have formed first at the symmetry plane, unlike what the velocity profiles might seem to suggest. (This assumes, reasonably, that the second order derivatives are not zero at the extremum.) Indeed, examination of the streamwise shear contours (not presented here) shows that two negative shear extrema are located at symmetric positions somewhat away from the center line.

Going from station 2 to station 3, the (scaled) streamwise vortices gather even more strength. On the other hand, the strength of the wall vorticity decreases. As a result, the vortices away from the wall take over as the locations of the strongest vorticity. The values of the extrema are plotted as the dashed lines in the center graph in Fig. 2(c).

The vortices at station 3 have also become quite compact. Looked at inviscidly, their close proximity to each other would mean that their effects cancel each other significantly over most of the domain. The wall pressure distribution has become remarkably flat, Fig. 2(d), making the wall pressure gradient almost zero away from the center plane.

Going to station 4, the vortices diffuse out some and a significant spanwise pressure variation reestablishes itself. Once again, this pressure distribution tends to drive the fluid near the wall toward the center plane. The wall shear at the center plane stops evolving toward the spanwise average and decreases again a bit.

Around station 4, the boundary layer thickness has grown to be comparable to the spanwise scale. In terms of inviscid vortex motion, the streamwise vortices are now well separated from their mirror images below the wall. Their inviscid effect on the flows near the ends of the period is to stretch the spanwise vorticity and draw higher-momentum fluid closer to the wall. Near the center plane, however, they compress the spanwise vorticity and contribute to a motion away from the wall. Consistent with this picture, going to station 5, the wall shear in the center plane is observed to stagnate, Fig. 2(b). On the other hand the wall shear near the ends of the period grows quite significantly. Around station 6, the location of separation without blowing, the wall shear near the ends extends well above the Blasius value for zero adverse pressure gradient. And all velocity profiles have been energized enough that they are well clear from separating.

The boundary layer is now getting quite thick compared to the spanwise scale, suggesting that spanwise diffusion will become a dominating effect. The rise in wall shear at the center plane from station 5 to station 6 is consistent with an increasing importance of

spanwise diffusion. And so is the rapid and apparently exponential decay of all three-dimensional flow features between stations 6 and 7. In any case, at station 7, the velocity profiles are fully two-dimensional, although still well away from a Blasius profile. And all contour lines of streamwise vorticity have disappeared.

7. Autogenous suction

Atik and Van Dommelen [13] showed that in two-dimensional flow, separation can theoretically be eliminated by "autogenous suction", boundary layer suction driven by the adverse pressure gradient that causes the separation. In the scheme, the fluid that is sucked away where separation wants to occur is ducted toward the lower pressure region farther upstream of separation. Since boundary-layer suction volumes are asymptotically small, the head loss can be asymptotically small. On the other hand boundary layers can support a finite, though numerically small, pressure drop. There is much less hydraulics involved in ducting the fluid a small fraction of the chord upstream than to duct the fluid all the way along the wing span toward a pump in the fuselage, as has been done in more conventional applications. However, [13] do find that the blowing distribution needs to be very precisely tuned to prevent the upstream blowing to cause separation before the downstream suction has picked up enough strength to prevent it.

This raises the question whether autogenous suction could be used in the current framework. It could circumvent the need in the two-dimensional case to finish all blowing before suction can start. In three dimensions, fluid can be ducted spanwise and ejected at a station only slightly upstream and only a boundary-layer thickness scale distance away in the spanwise direction. Both the suction and the blowing could then contribute to generating the streamwise vortices that are to prevent the separation. Such a scheme is likely to be more robust to small flow changes than the two-dimensional one.

As a proof of concept, in this section a limiting case will be examined in which the head loss for the ducted fluid is assumed to be zero. Thus the fluid is ejected at the same streamwise position as it is sucked away. This case can be done using the same blowing distribution (19) as in the previous section if its spanwise average is subtracted.

It turns out, maybe not surprisingly, that it is easier to remove separation with a combination of suction and blowing than with pure blowing. While we did not succeed in eliminating the need for negative wall curvature completely, we did manage to reduce its magnitude by a factor 4. At the same time we reduced the blowing velocity (before subtracting the average) by a factor 2.

As Fig. 4(b) shows, with these reductions in boundary-layer manipulation we did get quite close to separation in the region where the two-dimensional boundary layer separates. However, the near-separation in the initial region is gone, and with it the associated complex dynamics. Qualitatively, Figs. 4 and 5 are not unlike Figs. 2 and 3, but note the very different numbers on the axes and contours.

It should of course be noted that for practical application, the microjet scheme is significantly simpler. This is especially so because a source of high pressure air is often readily available, e.g., from the aircraft engines.

8. Discussion

8.1. Conclusion

This paper was concerned with the effect of small-volume transverse blowing on laminar boundary-layer separation. In particular, the case of three-dimensional blowing into an otherwise two-dimensional incompressible boundary layer was addressed.

Fig. 4. Like Fig. 2, but for spanwise-alternating blowing and suction.
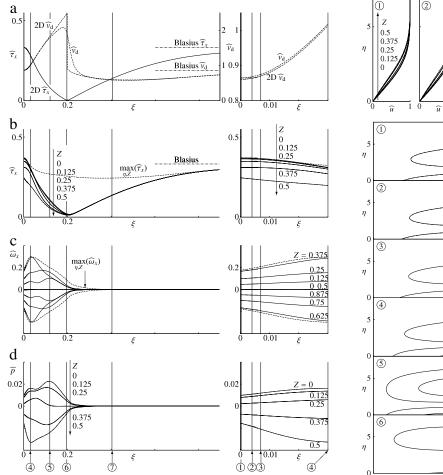

Fig. 5. Like Fig. 3, but for spanwise-alternating blowing and suction.

The blowing was assumed to stay within the normal small transverse boundary layer scale. The most interesting result for practical purposes was to show that in at least some circumstances, such blowing can remove separation. However, blowing that can validly be described by the normal three-dimensional boundary-layer equations will not do so. Such blowing will only promote separation. To be able to remove separation, a blowing distribution is needed that varies nontrivially in the spanwise direction on the short Görtler scale.

The numerical results indicate that the beneficial effects are due to the enhanced mixing by streamwise, Görtler scale, vortices. As is well known, such vortices, while small in the cross plane, persist for finite distances downstream. While the use of streamwise vortices to eliminate separation is well established, the current results manage to do so while staying fully within boundary layer scalings. The generated drag stays small of order $Re^{-1/2}$ like in a normal attached laminar boundary layer.

These Görtler-scale flows are quite hard to compute numerically. A new scheme was formulated to allow for the various problem areas.

According to the present results, an equal combination of blowing and suction, such as in asymptotic autogenous suction, is more effective than blowing alone.

What is the nature of the Görtler-scale boundary-layer solution when an attached flow does not exist is not yet clear. Numerical results so far suggest that the Görtler-scale boundary-layer solution remains nonsingular as long as the streamwise wall shear does not reverse. In the absence of singularity, a self-consistent high R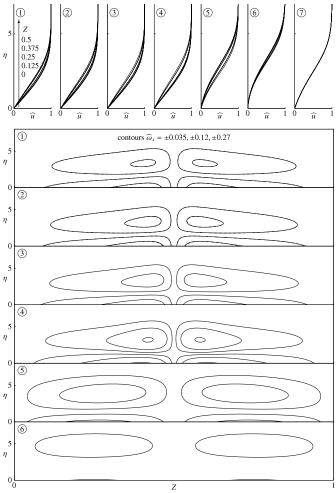eynolds number composite solution consisting of an attached potential flow and a thin boundary layer at the wall exists. Following Sears and Telionis [17], such flows should be defined to be unseparated for physical reasons. The numerical results of Appendix B suggest that if an attached solution does not exist, there may be a singularity in the region of reversed flow in the Görtler-scale boundary-layer solution. However, this result is obtained by extrapolation. The downstream-marching boundary layer problem is improperly posed for reversed streamwise wall shear, and code modifications would be needed to explore the region beyond zero wall shear.

8.2. Additional remarks

Interesting as the above results may be, a primary objective of this study was to create a simple model to gain some understanding of flow control by microjets. Now that such a model has been established, some insight may become possible. For example, if the experiments and the model agree, some more abstract understanding of the mechanics may have been obtained. On the other hand, if experiments and the model disagree, the question "Why?" can be raised. This too is likely to increase understanding.

The current results are still very limited. Only a couple of examples have been computed so far. But one conclusion of all the numerical experimenting done to achieve these examples is that it is not really that easy to achieve effective separation control in laminar flow in the described way. Surely not as easy as it is experimentally in turbulent boundary layers. The initial, quasi-two-dimensional, effect of blowing on separation is adverse. Farther

downstream there may be a beneficial effect, but it first needs to overcome what is left of the earlier adverse effects. Our numerical observations are that the streamwise vortices tend to diffuse away before they have the time to do much good. In both successful cases we had to assume a slightly concave wall, in which the Görtler instability mechanism helps to keep the vortices alive.

That obviously raises the question why this seems less of an issue in turbulent flows, (e.g. [1,6]). It may be that the higher average velocity of a turbulent velocity profile plays a part. Recall that for a constant streamwise velocity, the Görtler equations become the two-dimensional unsteady Navier–Stokes equations, with the streamwise coordinate taking the place of "time". If the streamwise velocity is higher, the "time" available for diffusion until the flow reaches a given downstream location is less. Also, when the variation in streamwise velocity is smaller, the vorticity becomes more streamwise, reducing three-dimensional vortex mechanics that conceivably might disrupt the vortices. (The cross-plane gradients of the streamwise velocity produce the nonstreamwise vorticity components.) Including a turbulence model in future computations might be a way to get some more insight in this issue. (An unreported study of the effect of variable viscosity on the *initial* flow was in fact conducted. The conclusion was that it did not make much of a difference. But there does not seem to be a good reason why it should for the initial flow.)

Note that the fact that so far we have not succeeded in removing separation from flat and convex walls does not mean it cannot be done. Clearly Görtler vortices will provide cross-plane mixing whether the wall is concave or convex. In that respect, there is no fundamental difference in the equations of motion for concave and convex walls. In either case, the Görtler vortices have a finite length in the streamwise direction. The difference in length is quantitative rather than qualitative. The numerical problem was to create vortices that avoided zero wall shear in the region of blowing and that remained strong enough traveling down to separation. In experiments, a limited amount of "separation", i.e. reversed streamwise flow, near the microjets may be fine. However, the computations have to stay below the blowing level that creates reversed flow or they become improperly posed. That limits the blowing that can be applied. But in fact, the present computations could not even reach the blowing level that produces zero wall shear. They were limited by numerical resolution in resolving the strong initial gradients in the initial near-separation caused by the blowing. If separation could be approached more closely, the strong vorticity ejection of Fig. 3 should strengthen still further.

Another issue is how well the used blowing distribution simulates microjets. The relative spanwise size of the blowing distribution was a much larger fraction of the period than in the experiments. So was the streamwise size. The true microjet scale would produce severe numerical resolution problems. However, sharpening the blowing distribution might introduce stronger jet entrainment. Such entrainment might act much like suction to remove the low momentum fluid near the wall. And recall from Section 7 that a combination of suction and blowing is considerably more efficient than blowing alone.

Note also that according to the two-dimensional unsteady flow analogy, the present computations barely seem to scratch the surface. As seen in the cross plane, the computed transverse flows are clearly low Reynolds number ones, where all relevant features have the scale of the period. All the potential richness of high Reynolds number cross-plane flows remains to be explored.

Another issue that may be important is the vortex stretching found near, say, a front stagnation point. Conceivably this might be another way besides wall curvature to keep the streamwise vortices alive until they can do something beneficial. All computations so far have been started from a Blasius-like boundary layer in which such stretching is absent. Future studies should look at stagnation-point flows.

A final area that needs more attention is spanwise flow above the boundary layer. Since the cross-flow scaling is small, such spanwise flow might have a dramatic impact. The presented results paid relatively little attention to cross flow since in initial exploratory studies, zero cross flow seemed to work best. Note that [66] did find that cross flow can at least locally produce a beneficial effect, possibly by stirring up the vortex mechanics. However, these computations did not use the Görtler instability mechanism, which might possibly be adversely affected by cross flow, [50,67]. In addition, the current study attempted to simulate the effect of microjets, which will drift downstream with the boundary layer fluid.

During the course of this study, the experimental work of [68] became available. Their conclusions about the formation of streamwise vortices and their beneficial effects seem very similar to those of the present study.

Acknowledgments

Appendix A. Some data about the numerical solution

This appendix summarizes basic data about the numerical solution. Note that many of the parameters below were chosen based on heuristic arguments and trial and error.

For the computations of Sections 6 and 7, the streamwise computational coordinate was defined as:

$$\alpha = \frac{1}{\pi} \arctan \sqrt{\frac{x}{l_{1\alpha}}} + \frac{1}{\pi} \arctan \sqrt{\frac{x}{l_{2\alpha}}} \quad l_{1\alpha} = 0.01 \quad l_{2\alpha} = 5. \text{ (A.1)}$$

This puts half the streamwise mesh points in a range of order 0.01, and the other half in a range of order 5. The square roots remove the singularity that would otherwise exist in the solution at $x = 0$. The spanwise coordinate was

$$Z = \frac{z}{\lambda} = \gamma + \frac{f_\gamma}{2\pi} \sin(2\pi\gamma) \quad f_\gamma = 0.66. \tag{A.2}$$

The sine term increases the resolution at the center of the period, where the blowing peaked. The transverse coordinate was

$$\beta = (1 - f_\beta) \frac{2}{\pi} \arctan\left(\frac{2\pi y}{f_\lambda \lambda}\right) + f_\beta \frac{2}{\pi} \arctan\left(\frac{y}{D(x)}\right) \tag{A.3}$$

$$f_\beta = 0.625 \quad f_\lambda = 0.69.$$

This spreads a fraction $1 - f_\beta$ of the mesh points over a length scale comparable to the period. The remaining fraction f_β of mesh points is spread over a scale $D(x)$, taken as a crude estimate for the viscous boundary layer thickness:

$$D(x) = C_D \sqrt{x} \left\{ 1 + \frac{f_D}{1 + (x - x_D)^2 / l_D^2} \right\} \tag{A.4}$$

$$C_D = 4.41 \quad f_D = 1 \quad x_D = 6.2 \quad l_D = \frac{1}{2} x_D.$$

To keep the computational unknowns finite, they were defined as follows:

$$U = \frac{u}{R(x)} \quad V = S(x)v - C_V V_0 \left(\frac{y}{D(x)}\right) \quad W = S(x)w \tag{A.5}$$

$$P = T(x)p - C_P D(x)P_0 \left(\frac{y}{D(x)}\right) \quad K = R^2(x)S^3(x)\kappa. \tag{A.6}$$

Here $R(x) = 1$, $S(x) = \sqrt{x}$, and $T(x) = D^2 S$ are chosen functions that can be modified based on the type of flow computed. Functions V_0 and P_0 with their coefficients capture the blow up of v and $p_{,y}$ at large y:

$$V_0 = \ln\left(\cosh\frac{y}{D}\right) \sim \frac{y}{D} - \ln 2$$

$$C_V = -RDS\alpha_{,x}U_{e,\alpha} - R'DSU_e$$
(A.7)

$$P_0 = \frac{1}{2}V_0^2$$

$$C_P = \frac{RT}{S}\left\{\left(\frac{D'}{D} + \frac{S'}{S}\right)C_V - \alpha_{,x}C_{V,\alpha}\right\}U_e - \frac{T}{DS^2}C_V^2.$$
(A.8)

The transformed momentum equations can be straightforwardly rewritten in terms of these new coordinates and variables.

It is desirable that U and W approach the exact U_e and W_e at infinite y. This avoids accumulation of errors in the external flow boundary condition and simplifies code logic. It can be achieved by evaluating the streamwise derivatives of the external flow by the same difference scheme as used for the velocities inside the boundary layer. Then it is seen from the governing equations that the variables V and $P_{,y}$ approach constants too.

All streamwise, α, derivatives were discretized using the backward, second order, A-stable finite difference formula. Our experience with boundary layer computations is that the implicit viscosity in this discretization avoids oscillations that may occur in Crank–Nicholson type discretizations in the presence of abrupt changes in wall transpiration velocity, [12,13]. The α derivatives drop out at the start of the plate, allowing the appropriate initial conditions to be found iteratively by solving ordinary difference equations in the β direction. This is preferable to putting in the exact initial conditions, which would produce a relatively large error, [28].
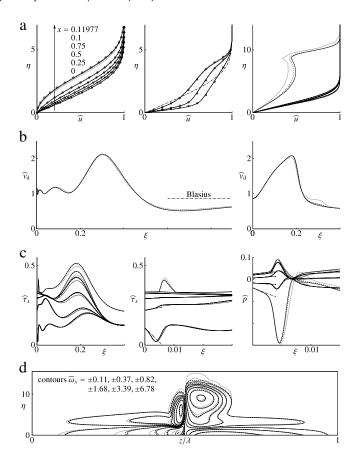
Because the y stretching is in places very nonlinear, dependent variables that vary accurately linearly or quadratic with y may vary very nonlinearly with β. Therefore, to maintain meaningful values for the y derivatives everywhere, they were evaluated in terms of y instead of in terms of β. The same scheme was also used for the γ derivatives. An additional modification was made to the convective γ-derivatives. These were approximated as

$$C_\gamma f_{,\gamma} - \frac{1}{2}\Delta\alpha\Delta\gamma\left|C_\gamma\right|f_{,\alpha\gamma\gamma} \quad \text{for } f = U, V, W$$
(A.9)

using the normal second order γ differences and a first order backward α difference. This discretization produces a diagonally-dominant bidiagonal formula for the f-values in the current plane, which aids the convergence of the used symmetric Gauss–Seidel iterations in the γ-direction. The beta derivatives were evaluated using central differences in the regions of normal variation of mesh size. In the regions of singular or near singular variation of mesh size, a limited amount of upwinding was used. It was demanded that the upwinding did not increase the formal truncation error by more than 50%.

To obtain a good cross-plane discretization of the continuity equation, the pressure and spanwise velocity location were staggered in the cross-plane mesh like in a two-dimensional unsteady MAC scheme [69]. The cross-plane pressure derivatives in the momentum equations and the velocity differences in the continuity equation were evaluated correspondingly.

Fig. A.6 shows various data relevant to numerical accuracy. All computations in this paper were conducted at three different mesh sizes and two cut-off values so that their accuracy could be verified. (The results at the two values of the cut-off are invariably for all practical purposes indistinguishable. It may also be mentioned that because of the coarse spacing in the top of the viscous region, the

Fig. A.6. Tests on numerical accuracy using three mesh sizes, coarse (dots), medium (short dash), and fine (solid). The medium curves show results for two different cutoffs (indistinguishable). See the text for details.

actual mesh point at which the switch from viscous to inviscid equations is made is typically only one unit different.)

The top left velocity profiles provide a first sanity check. They show Howarth flow, [70], as computed using the present scheme. This is a two-dimensional flow with an external flow given by $u_e = 1 - x$. The current scheme used mesh sizes 96,36,2/7 192,72,2/7, 192,72,2/9, and 384,144,2/7. These represent streamwise, transverse, and spanwise mesh points respectively, with the value of the y/D cut-off following the slash. Quadratic convergence with mesh size is observed, and only the separation profiles show some noticeable differences between meshes. Symbols are the results of Howarth. These are impressively accurate for a computation done in 1938. (The Howarth values for the final separated velocity profile are at $x = 0.12$).

The velocity profiles in the top center of Fig. A.6 provide a sanity check for a three-dimensional nonlinear case. Good quantitative agreement exists with the velocity profiles computed by Hall for the same flow, [52, Fig. 3(c)]. The mesh sizes in this computation were 256,64,16/10, 512,128,32/10, 512,128,32/8, and 1024(2048),256,64/10. (For the finest mesh, the iterative procedure would not converge at the position 100 where the strong perturbation is impulsively applied. As a simple fix, the streamwise mesh was doubled from that point on.) Note that this computation and the Howarth one used somewhat different mesh stretchings than the ones described above.

The remaining plots in Fig. A.6 apply to the main computations of this paper in Sections 6 and 7, in particular Figs. 2–5. The plots in Fig. A.6 show the parts of these figures where notable differences between the meshes were found. The meshes were 256,48,64/8, 512,96,128/8, 512,96,128/10, and 1024,192,256/8.

First, the velocity profiles top right in Fig. A.6 are at an early stage in which strong, peaked blowing is applied. This blowing nearly causes separation. The velocity profile on top of the blowing peak gets blown far up, to where the viscous mesh resolution becomes low. As a result, the coarsest mesh has clear difficulty resolving the top part of the velocity profile. However, quadratic convergence with mesh size is observed and the finest mesh should be accurate to approximately line thickness.

Part (b) of Fig. A.6 shows the displacement velocity for the cases of Sections 6 and 7, respectively. In the latter plot it is seen that the coarsest mesh really struggles at the point where the boundary layer gets very close to a marginal separation. Again, the finest mesh seems to be accurate to approximately line thickness. It may be noted that this is the only place where the differences between meshes are worth mentioning for the results of Section 7. All remaining plots pertain to Section 6.

Part (c) of Fig. A.6 shows the streamwise wall shear on two streamwise scales and the cross-flow wall pressure distribution. Broken lines are a second-order asymptotic theory for small ξ. Note that the initial conditions away from the boundaries are not prescribed but computed on the finite difference mesh. Therefore both the agreement in value with theory and the one in slope are nontrivial. The results are seen to agree very well with theory. Unfortunately, theory has only a very limited range of applicability. The wall shear quickly drops below the theory and suffers the near-separation mentioned earlier. At about that time the coarsest mesh also suffers resolution problems in computing the pressure and wiggles develop. These disappear for the finer meshes and once again the finest mesh seems to be accurate approximately to line thickness.

Part (d) of Fig. A.6 shows contour lines of streamwise vorticity in two cross-flow planes at the near-separation. Again the coarse mesh shows quite noticeable deviations while the finest mesh is again accurate approximately to line thickness. Note also the poor behavior of the coarsest mesh far from the wall. However, these are quite small values of the vorticity in the near-potential region where the vorticity is almost constant at zero. (The shown contour lines are densely spaced around zero, the line of largest vorticity having 60 times the vorticity of the one of lowest vorticity.)

Except for these cases where the accuracy is approximately equal to line thickness, the results in Sections 6 and 7 seem to be accurate to within line thickness.

Appendix B. The Goldstein singularity and blowing

According to numerous numerical computations, in two-dimensional flow, an incompressible boundary layer terminates in a Goldstein singularity at flow reversal for a prescribed external flow with a sufficiently adverse pressure gradient. Then following [24] the obtained boundary layer solution is not physically meaningful except as a signal that the assumed higher Reynolds number solution with an attached external flow does not exist.

To be sure, there are some exceptions to the above statement. First, [25] showed that for a pressure–displacement law different from a thin boundary layer below a potential flow as assumed here, the singularity may be removable.

Second, it is in principle possible to have zero wall shear without a Goldstein singularity. The simplest example is, of course, the Falkner–Skan separation profile. This special solution has the wall shear zero everywhere. There is no singularity except at the start of the boundary layer. More generally, at zero wall shear an asymptotic expansion exists that is nonsingular, [22].

Catherall and Mangler [71] argue that nontrivial solutions of this kind can in fact be created, by the trick of prescribing the displacement thickness instead of the pressure near and in the reversed flow region. Physically these would correspond to attached flow in the sense of Section 2; while there is reversed flow in the asymptotic thin boundary layer, the asymptotic external flow is the attached one for that body. However, the velocity and displacement thickness boundary conditions used by Catherall and Mangler are, as noted by [24], rather artificial and contrived. No actual bodies corresponding to these solutions were identified. More work is needed to understand why such solutions have so far not been observed numerically for given bodies.

Third, a marginal case of the Goldstein singularity exists. The marginal case occurs when the flow around a body is initially unseparated, and the flow parameters then changed to produce a more adverse pressure gradient. Ruban [58,59] and independently Stewartson et al. [60] showed that when the first point of zero wall shear appears, the singularity is of a degenerate type. More importantly, they showed that in an asymptotically small parameter range around the critical ones, a small thin reversed flow region can exist in the boundary layer region due to viscous–inviscid interaction.

If nonsingular solutions as described by Catherall and Mangler [71] would show up numerically for prescribed external flows, it would weaken the arguments of Section 3. Then it would be conceivable that while the blowing moves zero wall shear upstream, it might also change the boundary layer into a nonsingular one. Such a flow would then be unseparated in the terminology of Section 2, though still "separated" in the classical sense. More study is needed to address this concern.

As far as marginal separation is concerned, surely it should be possible to create such a separation upstream of the original one by blowing. However the flow would remain separated because of the singularity downstream.

Within the context of the present numerical study, it may be interesting to examine the effect of three-dimensional blowing on the singularity itself. In particular, the results of this section will suggest that for Görtler-scale blowing, a thin reversed flow region of finite length may occur.
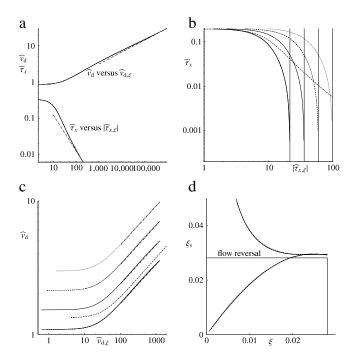
As mentioned in Section 3, if the spanwise scale of the blowing exceeds the Görtler scaling, the flow is quasi-two-dimensional. So then a Goldstein singularity will form at the first point where the streamwise shear reaches zero. At other spanwise locations, the boundary layer computation can be continued farther downstream. (However, the analysis of [24] applied at the first point of zero wall shear suggests that the obtained solution is physically not meaningful and that the assumed attached flow simply does not exist.)

The above does not apply for a Görtler spanwise scaling. Here different spanwise locations interact through spanwise diffusion. As a result, the computation at all spanwise locations will become improperly posed beyond the first point of reversed streamwise flow. But intuitively it seems hard to imagine that the flow over the entire span separates in the two-dimensional manner if just a single point reverses. A weaker separation process seems more likely. Since neighboring spanwise positions are linked, this suggests that even at the reversal point, the singular behavior may be weaker than in two-dimensional flow.

In order to understand this better, we performed a trial computation of a Howarth [70] type flow. In such a flow, the constant external flow of Blasius is replaced by $u_e = 1 - x$. This creates an adverse pressure gradient that without blowing produces separation at $x = 0.120$. Fig. A.6 showed the two-dimensional velocity profiles without blowing, as computed using the current numerical scheme.

The wall shear becomes zero at the separation point, but its gradient blows up. In particular, if $\Delta\xi$ is the distance in terms of ξ to separation, the wall shear is asymptotically proportional to $\sqrt{\Delta\xi}$, [22,39,40]. Therefore, if the wall shear is plotted against the wall shear gradient on a double-logarithmic scale, asymptotically the curve will approach a line of slope -1. This is shown in Fig. B.7(a). The displacement velocity blows up as $1/\sqrt{\Delta\xi}$, so its corresponding plot has an asymptotic slope $\frac{1}{3}$.

Fig. B.7. Effect of three-dimensional blowing on the Goldstein singularity. Meshes are 96,36,36/7 (dots), 192,72,72/7 and 192,72,72/9 (short dashes), and 384,144,144/7. Long dashes indicate the quasi-two-dimensional solution valid for long scaled period.

Table C.1
Pohlhausen parameter that causes separation at various mesh sizes.

Mesh	K_s
256×30	-0.076471
512×60	-0.076465
1024×120	-0.076435
2048×240	-0.076420
4096×480	-0.076416
8192×960	-0.076414

The numerical results, as computed using the present scheme, agree well with these predictions. Fig. B.7(a) shows results for three different mesh sizes. It should additionally be noted that the streamwise mesh was several times doubled when approaching the point of zero shear. For the smallest wall shear values, differences between the three meshes become visible. However, as long as the results are mesh-independent, they are seen to follow the expected theoretical slope.

To examine the effect of three-dimensional blowing, a simple blowing distribution of the form

$$\widehat{v}_{w0} = 0.1 \left(1 - \cos \frac{2\pi \widetilde{z}}{\widetilde{\lambda}} \right) \tag{B.1}$$

was added, using the variables as defined in Section 6.

The first flow reversal for this blowing distribution occurs at the center period, where the blowing velocity is largest. However, as Fig. B.7(b) shows, the wall shear gradient remains finite at flow reversal in the absence of blowing. The figure shows the three meshes both superimposed, as well as shifted apart so that they can be seen independently. There are no significant differences between the meshes. In fact, all three meshes agree on the location of the flow reversal and the wall shear slope at that location to three digits accurate.

Fig. B.7(b) also shows the quasi-two-dimensional solution valid for large scaled period. This solution separates earlier, with a normal Goldstein behavior. Not only does the Görtler scaling shift

the flow reversal downstream, it also eliminates the square root singularity when it does occur.

Fig. B.7(c) shows the displacement velocity with Görtler-scale blowing. The behavior is similar to the Goldstein case, (shown as the long dashes for the long scaled period case). However, the slope seems to be somewhat smaller. A slope of $-5/12$ is shown as the dot–dash lines.

Assuming a constant value for the slope, the displacement velocity and its derivative at a given location ξ can be used to extrapolate a location ξ_s where the displacement velocity would become singular. These extrapolated locations are shown in Fig. B.7(d). In the top curve, the slope was assumed to be $-5/12$. In the lower curve, the slope is taken to be the local derivative $\mathrm{d} \left(\ln v_d \right) / \mathrm{d} \left(\ln v_{d,\xi} \right)$. Both curves seem to predict a singularity that is a finite distance beyond the initial flow reversal point.

These results suggest that the flow may only become singular a finite distance behind the first flow reversal. If so, local manipulation, such as suction, might be applied near the singular point to prevent the singularity. That then raises the possibility that there might be attached flows with a finite region of reversed flow on Görtler scalings. This would be different from the case of marginal separation in two-dimensional flow, [58–60], where the reversed flow region is asymptotically small.

Appendix C. External flow for marginal separation

The Pohlhausen approximation of the boundary layer equations, in the form of Holstein & Bohlen, and simplified by Walz, [44, Eq. (10.37)], can be written as

$$K = \frac{a}{b-1} \frac{\Phi}{\Phi'} \frac{\mathrm{d}\Phi'}{\mathrm{d}\Phi} \quad a \approx 0.47 \quad b \approx 6 \tag{C.1}$$

where primes denote differentiation with respect to the streamwise coordinate x, K is a nondimensional parameter governing the shape of the velocity profile, and Φ is an integral of the velocity:

$$K \equiv u_e' \frac{\delta_2^2}{\nu} \qquad \Phi(x) \equiv \int_{\underline{x}=0}^{x} u_e^{b-1}(\underline{x}) \, \mathrm{d}\underline{x} \tag{C.2}$$

where δ_2 is the boundary layer momentum thickness and ν the viscosity.

Note that since normally only a relatively small drop in external flow velocity is sufficient to produce separation, Φ is roughly speaking proportional to x. Therefore, if the shape parameter K is chosen to be a suitable function of Φ, it will be a similar function of x. But choosing K as a function of Φ instead of x has the advantage that (C.1) may be integrated by separation of variables.

In this study, we chose

$$K = K_s \Phi e^{1-\Phi}. \tag{C.3}$$

This has K zero, corresponding to Blasius flow, both at the start of the plate and infinitely far downstream. At $\Phi = 1$, however, an extremal value K_s is reached. The expression above has the advantages that the shape of the velocity profile immediately starts evolving to the separated one, and that the shape far downstream is exponentially close to the Blasius one. In addition, it allows (C.1) to be integrated analytically.

Theoretically, marginal separation would occur when taking $K_s = -0.1567$, the separation value, [44, p. 212]. However, the accuracy of the Pohlhausen approximation near separation is low, and the true flow separates earlier, (cf. [44, Fig. 10.7]). Indeed, boundary layer computations show that marginal separation occurs at $K_s = -0.07641$, Table C.1. In the three-dimensional computations, $K_s = -0.0765$ was used to make sure that the corresponding two-dimensional flow is indeed separated. We could easily have increased the magnitude of this parameter further, but that would involve making an arbitrary choice for that

value. The logical value is surely as close as possible to the marginal value, but still high enough that the two-dimensional flow is definitely separated in the sense of Section 2.

The actual position of separation is at $x = 2.91$ or $\xi = 0.199$. (The Pohlhausen approximation would give separation at $x = 7.09$ for the theoretical K_s, or minimum shear at $x = 2.43$ for the actual K_s.)

References

[1] C. Shih, J. Beahn, A. Krothapalli, M. Chandrasekhara, Control of compressible dynamic stall using microjets, in: FEEDSM2003-45627, 4th ASME-JSME Joint Fluids Engineering Conference, ASME, 2003.

[2] V. Kumar, F.S. Alvi, Use of supersonic microjets for active separation control in diffusers, in: 33rd AIAA Conference and Exhibit, AIAA, 2003, Paper 2003-4160.

[3] V. Kumar, F.S. Alvi, Efficient control of separation using microjets, in: 35rd AIAA Conference and Exhibit, AIAA, 2005, Paper 2005-4879.

[4] V. Kumar, F.S. Alvi, Use of high-speed microjets for active separation control in diffusers, AIAA 44 (2006) 273–281.

[5] E. Fernandez, R. Kumar, F.S. Alvi, Effect of microjet spacing on the control of a highly separated flowfield, in: 6th AIAA Flow Control Conference, AIAA, 2012, Paper 2012-2348.

[6] E. Fernandez, R. Kumar, F.S. Alvi, Separation control on a low-pressure turbine blade using microjets, AIAA J. Propulsion Power (2013).

[7] G. Lachmann (Ed.), Boundary Layer and Flow Control, Volume I, Pergamon Press, London, 1961.

[8] G. Lachmann (Ed.), Boundary Layer and Flow Control, Volume II, Pergamon Press, London, 1961.

[9] R.A. Wallis, The Use of Air Jets for Boundary Layer Control, Technical Report Aero Note 110, Aerodynamics Research Laboratories, Australia, N-34736, 1952.

[10] J. Johnston, M. Nishi, Vortex generator jets-means for flow separation control, AIAA J. 28 (1990) 989–994.

[11] L. Prandtl, Über Flüssigkeitsbewegung bei sehr kleiner Reibung, in: Verhandlungen des III. Internationalen Mathematiker-Kongresses, Heidelberg 1904, Teubner, Leipzig, 1905, pp. 484–491. Also in "Ludwig Prandtl gesammelte Abhandlüngen", Springer-Verlag, 1961.

[12] H. Atik, C.-Y. Kim, L. Van Dommelen, J. Walker, Boundary-layer separation control on a thin airfoil using local suction, J. Fluid Mech. 535 (2005) 415–443.

[13] H. Atik, L. Van Dommelen, Autogenous suction to prevent boundary layer separation, J. Fluids Engineering 130 (2008) 011201–1 to 8.

[14] K. Stewartson, C. Simpson, On a singularity initiating a boundary-layer collision, Quart. J. Mech. appl. Math. 35 (1982) 1–16.

[15] W. Banks, M. Zaturska, The collision of unsteady laminar boundary layers, J. Engineering Math. 13 (1979) 193–212.

[16] L.L. Van Dommelen, On the Lagrangian description of unsteady boundary-layer separation. Part 2. The spinning sphere, J. Fluid Mech. 210 (1990) 627–645.

[17] W.R. Sears, D.P. Telionis, Boundary-layer separation in unsteady flow, SIAM J. Appl. Math. 23 (1975) 215–235.

[18] F. Moore, On the separation of the unsteady laminar boundary layer, in: H. Görtler (Ed.), Boundary-Layer Research, Springer, 1958.

[19] N. Rott, Theory of time-dependent laminar flows, in: F. Moore (Ed.), Theory of Laminar Flows, Princeton, 1964, pp. 395–438.

[20] W. Sears, Some recent developments in airfoil theory, J. Aeronaut. Sci. 23 (1956) 490–499.

[21] J.I. Williams, Incompressible boundary layer separation, Ann. Rev. Fluid Mech. 9 (1977) 113–144.

[22] S. Goldstein, On laminar boundary-layer flow near a position of separation, Quart. J. Mech. Appl. Math. 1 (1948) 43–69.

[23] H. Blasius, Grenzschichten in Flüssigkeiten mit kleiner Reibung, Z. Math. Phys. 57 (1908) 1–37.

[24] K. Stewartson, Is the singularity at separation removable? J. Fluid Mech. 44 (1970) 347–364.

[25] F.T. Smith, P.G. Daniels, Removal of Goldstein's singularity at separation, in flow past obstacles in wall layers, J. Fluid Mech. 110 (1981) 1–37.

[26] V.V. Sychev, Laminar separation, Izv. Akad. Nauk. SSSR, Mekh. Zhid. i Gaza 3 (1972) 47–59.

[27] F.T. Smith, The laminar separation of an incompressible fluid streaming past a smooth surface, Proc. Roy. Soc. A 356 (1977) 443–463.

[28] L.L. Van Dommelen, S.F. Shen, The spontaneous generation of a singularity in a separating boundary layer, J. Comput. Phys. 38 (1980) 125–140.

[29] S. Cowley, Computer extension and analytic continuation of Blasius expansion for impulsive flow past a circular cylinder, J. Fluid Mech. 135 (1983) 389–405.

[30] L.L. Van Dommelen, S.F. Shen, The genesis of separation, in: T. Cebeci (Ed.), Symposium on Numerical and Physical Aspects of Aerodynamic Flows, Springer-Verlag, 1982, pp. 293–311.

[31] L.L. Van Dommelen, Unsteady Boundary Layer Separation, Ph.D. Thesis, Cornell University, 1981.

[32] J.W. Elliott, S.J. Cowley, F.T. Smith, Breakdown of boundary layers: (i) on moving surfaces; (ii) in semi-similar flow; (iii) in fully unsteady flow, Geophys. Astrophys. Fluid Dyn. 25 (1983) 77–138.

[33] V.V. Sychev, Asymptotic theory of non-stationary separation, Fluid Dyn. 14 (1980) 829–838. From Izv. Akad. Nauk. SSSR, Mekh. Zhid. i Gaza, 1979, 6, 21–32.

[34] L.L. Van Dommelen, S.F. Shen, An unsteady interactive separation process, AIAA J. 21 (1983) 358–362.

[35] G. Ludwig, An experimental investigation of laminar separtion from a moving wall, in: AIAA paper 64-6, AIAA Aerosp. Sci. Meeting, New York, 1964.

[36] O. Inoue, A numerical investigation of flow separation over moving walls, J. Phys. Soc. Japan 50 (1981) 1002–1008.

[37] O. Inoue, Mrs criterion for flow separation over moving walls, AIAA J. 19 (1981) 1108–1111.

[38] R. Yapalparvi, L. Van Dommelen, Numerical solution of unsteady boundary-layer separation in supersonic flow: upstream moving wall, J. Fluid Mech. 706 (2012) 413–430.

[39] K. Stewartson, On Goldstein's theory of laminar separation, Quart. J. Mech. Appl. Math. 11 (1958) 399–410.

[40] R.M. Terrill, Laminar boundary layer flow near separation with and without suction, Phil. Trans. Roy. Soc. A 253 (1960) 55–100.

[41] K. Nickel, Einige Eigenschaften von Lösungen der Prandtlschen Grenzschicht-Differentialgleichungen, Arch. Ration. Mech. Anal. 2 (1958) 1–31.

[42] K. Nickel, Prandtl's boundary-layer theory from the viewpoint of a mathematician, Ann. Rev. Fluid Mech. 5 (1973) 405–428.

[43] O. Oleînik, V. Samokhin, Mathematical Models in Boundary Layer Theory, Chapman & Hall/CRC, 1999.

[44] H. Schlichting, Boundary Layer Theory, seventh ed., McGraw-Hill, 1979.

[45] D. Catherall, K. Stewartson, P. Williams, Viscous flow past a plate with uniform injection, Proc. R. Soc. Lond. Ser. A 284 (1965) 370–396.

[46] L. Crocco, A Characteristic Transformation of the Equations of the Boundary Layer in Gases, Technical Report, Rep. Aero. Res. Coun., 1939.

[47] W. Walter, On the asymptotic behavior of solutions of the Prandtl boundary layer equations, Indiana Univ. Math. J. 20 (1971) 829–841.

[48] W. Rheinboldt, Zur Berechnung stationärer Grenzschichten bei kontinuierlicher Absaugung mit unstetig veränderlicher Absaugegeschwindigkeit, J. Rat. Mech. Anal., Indiana Univ. 5 (1956) 539–604.

[49] F.T. Smith, K. Stewartson, On slot injection into a supersonic laminar boundary layer, Proc. R. Soc. Lond. Ser. A 332 (1973) 1–22.

[50] P. Hall, Görtler vortices in growing boundary layers: the leading edge receptivity problem, linear growth and the nonlinear breakdown stage, Mathematika 37 (1990) 151–189.

[51] W. Saric, Görtler vortices, Annu. Rev. Fluid Mech. 26 (1994) 379–409.

[52] P. Hall, The nonlinear development of görtler vortices in growing boundary layers, J. Fluid Mech. 193 (1988) 243–266.

[53] K. Lee, J.T.C. Liu, On the growth of mushroomlike structures in nonlinear spatially developing Görtler vortex flow, Phys. Fluids A 4 (1992) 95–103.

[54] Y. Guo, W.H. Finlay, Wavenumber selection and irregularity of spatially developing nonlinear Dean & Görtler vortices, J. Fluid Mech. 264 (1994) 1–48.

[55] A. Benmalek, W.S. Saric, Effects of curvature variations on the nonlinear evolution of Görtler vortices, Phys. Fluids 6 (1994) 3353–3367.

[56] S.V. Patankar, D.B. Spalding, A calculation procedure for heat, mass and momentum transfer in three-dimensional parabolic flows, Int. J. Heat Mass Transfer 15 (1972) 1787–1806.

[57] L. Van Dommelen, A boosted p' method for fully parabolized flows, Numer. Heat Transfer 59 (2011) 245–258.

[58] A.I. Ruban, Singular solution of boundary layer equations which can be extended continuously through the point of zero surface friction, Izv. Akad. Nauk. SSSR, Mekh. Zhid. i Gaza (1981) 42–52. English translation: Fluid Dynamics, Vol. 16, Nov.–Dec. 1981, pp. 835–843.

[59] A.I. Ruban, Asymptotic theory of short separation regions on the leading edge of a slender airfoil, Izv. Akad. Nauk. SSSR, Mekh. Zhid. i Gaza (1982) 42–51. English translation: Fluid Dynamics, Vol. 17, Jan.–Feb. 1982, pp. 33–41. Translation has original paper as 1981.

[60] K. Stewartson, F.T. Smith, K. Kaups, Marginal separation, Stud. Appl. Math. 67 (1982) 45–61.

[61] H. Schlichting, K. Bussmann, Exakte Lösungen für die laminare Grenzschicht mit Absaugung und Ausblasen, Schr. Dtsch. Akad. Luftfahrtf. 7B (1943) 25–69.

[62] R. Iglish, D. Grohne, Die laminare Grenzschicht an der längsangeströmten ebenen Platte mit schrägem Absaugen und Ausblasen, Technical Report, Ber. Inst. Math. tech. Hochsch., Braunschweig 1/45, 1945.

[63] R. Iglish, Elementarer Existenzbeweis für die Strömung in der laminaren Grenzschicht zur Potentialströmung $U = u_1 x^m$ mit $m > 0$ bei Absaugen und Ausblasen, Z. Angew. Math. Mech. 33 (1953) 143–147.

[64] H.W. Emmons, D.C. Leigh, Tabulation of the Blasius Function with Blowing and Suction, Technical Report 157, Curr. Pap. Aero. Res. Coun., London, 1953.

[65] J.P. Hartnett, E.R.G. Eckert, Mass transfer cooling in a laminar boundary layer with constant properties, Trans. ASME 79 (1957) 247–254.

[66] H. Zhao, L. Van Dommelen, Manipulation of separation by transverse blowing, in: Ninth International Conference of Fluid Control, Measurement, and Visualization, 2007.

[67] A.P. Bassom, S.R. Otto, Weakly nonlinear stability of viscous vortices in three-dimensional boundary layers, J. Fluid Mech. 249 (1993) 597–618.

[68] S. Patil, T. Ng, Control of separation using spanwise periodic porosity, AIAA J. 48 (2010) 174–187.

[69] J.C. Tannehill, D.A. Anderson, R.H. Pletcher, Computational Fluid Mechanics and Heat Transfer, second ed., Taylor & Francis, London, 1997.

[70] L. Howarth, On the solution of the laminar boundary layer equations, Proc. R. Soc. Lond. Ser. A 164 (1938) 547–579.

[71] D. Catherall, K. Mangler, The integration of the two-dimensional laminar boundary-layer equations past the point of vanishing skin friction, J. Fluid Mech. 26 (1966) 163–182.